GPR119 Agonist AS1269574 Activates TRPA1 Cation Channels to Stimulate GLP-1 Secretion

Oleg G. Chepurny,* George G. Holz,* Michael W. Roe, and Colin A. Leech

Departments of Medicine (O.G.C., G.G.H., M.W.R., C.A.L.), Pharmacology (G.G.H.), and Cell and Developmental Biology (M.W.R.), State University of New York, and Upstate Medical University, Syracuse, New York 13210

GPR119 is a G protein-coupled receptor expressed on intestinal L cells that synthesize and secrete the blood glucose-lowering hormone glucagon-like peptide-1 (GLP-1). GPR119 agonists stimulate the release of GLP-1 from L cells, and for this reason there is interest in their potential use as a new treatment for type 2 diabetes mellitus. AS1269574 is one such GPR119 agonist, and it is the prototype of a series of 2,4,6 trisubstituted pyrimidines that exert positive glucoregulatory actions in mice. Here we report the unexpected finding that AS1269574 stimulates GLP-1 release from the STC-1 intestinal cell line by directly promoting Ca^{2+} influx through transient receptor potential ankyrin 1 (TRPA1) cation channels. These GPR119-independent actions of AS1269574 are inhibited by TRPA1 channel blockers (AP-18, A967079, HC030031) and are not secondary to intracellular Ca^{2+} release or cAMP production. Patch clamp studies reveal that AS1269574 activates an outwardly rectifying membrane current with properties expected of TRPA1 channels. However, the TRPA1 channel-mediated action of AS1269574 to increase intracellular free calcium concentration is not replicated by GPR119 agonists (AR231453, oleoylethanolamide) unrelated in structure to AS1269574. Using human embryonic kidney-293 cells expressing recombinant rat TRPA1 channels but not GPR119, direct TRPA1 channel activating properties of AS1269574 are validated. Because we find that AS1269574 also acts in a conventional GPR119-mediated manner to stimulate proglucagon gene promoter activity in the GLUTag intestinal L cell line, new findings reported here reveal the surprising capacity of AS1269574 to act as a dual agonist at two molecular targets (GPR119/TRPA1) important to the control of L-cell function and type 2 diabetes mellitus drug discovery research. (***Molecular Endocrinology*** **30: 614–629, 2016)**

Prescription medications that replicate the beneficial blood glucose-lowering actions of incretin hormone glucagon-like peptide-1 (GLP-1) are now recognized to be highly effective for the treatment of type 2 diabetes mellitus (T2DM) (1). These medications include the GLP-1 receptor agonists exenatide and liraglutide that stimulate pancreatic insulin secretion (2). They also include dipeptidyl peptidase-4 inhibitors such as sitagliptin and vildagliptin that slow metabolic degradation of GLP-1, thereby raising the levels of circulating GLP-1 substantially (3). Recently it became recognized that T2DM might also be treatable using orally administrable small molecules that directly stimulate GLP-1 release from intestinal L cells. For example, AR231453 is a GLP-1 secretagogue by virtue of its ability to activate the fatty acid amide receptor GPR119 expressed on L cells (4). Although it has yet to be demonstrated that T2DM can be treated with a GPR119 agonist, such preclinical findings provide a rationale for ongoing efforts to identify new GPR119 agonists that will act with increased efficacy and potency to stimulate GLP-1 release.

GPR119 is a G protein-coupled receptor that signals through G_S and adenylyl cyclase to increase levels of cAMP

ISSN Print 0888-8809 ISSN Online 1944-9917
Printed in USA

Received November 30, 2015. Accepted April 13, 2016.
First Published Online April 15, 2016

* O.G.C. and G.G.H. contributed equally to this work.

Abbreviations: AITC, allyl isothiocyanate; AKAR3, A-kinase activity reporter 3; $[Ca^{2+}]_i$, intracellular free calcium concentration; CRE, cAMP response element; ER, endoplasmic reticulum; EV, empty vector; FRET, fluorescence resonance energy transfer; GLP-1, glucagon-like peptide-1; GLU-Luc, glucagon gene promoter luciferase reporter; HEK-293, human embryonic kidney-293; IBMX, isobutylmethylxanthine; I-V, current-voltage; NSCC, nonselective cation channel; OEA, oleoylethanolamide; PKA, protein kinase A; RIP1, rat insulin 1 gene promoter; rTRPA1, rat TRPA1; SES, standard extracellular saline; T2DM, type 2 diabetes mellitus; TRPA1, transient receptor potential ankyrin 1; VDCC, voltage-dependent calcium channel; WT, wild type, YFP, yellow fluorescent protein.

so that L-cell GLP-1 secretion can be stimulated by GPR119 agonists such as AR231453 (5, 6). GPR119 also controls L-cell GLP-1 biosynthesis because it exerts a constitutive and ligand-independent action to stimulate proglucagon gene expression (7). Adding to this complexity, evidence exists that GPR119 signals through the G protein α-gustducin to stimulate GLP-1 secretion from L cells (8). When assessing these prior findings concerning GPR119, it is important to note that the pharmacological properties of available small molecule GPR119 agonists are not well understood. In fact, published studies indicate multiple molecular mechanisms of action for available GPR119 agonists (6). Furthermore, clinical studies of healthy or T2DM patients administered GPR119 agonists continue to provide disappointing outcomes for unexplained reasons (9). Therefore, there is a need to better understand the pharmacological properties and molecular mechanisms of action of small molecule GPR119 agonists.

AS1269574 is a small-molecule GPR119 agonist, and it serves as the lead compound for a series of 2,4,6 trisubstituted pyrimidines with potent GPR119 activating properties (10–15). Here the pharmacological properties of AS1269574 are investigated in greater detail using mouse GLUTag and STC-1 intestinal cell lines that serve as convenient model systems for the study of enteroendocrine cell function (7, 16–19). Using glucagon gene promoter luciferase (GLU-Luc) reporters in which luciferase expression is placed under the control of the proglucagon gene promoter (20), we report that AS1269574 stimulates proglucagon gene expression that constitutes an essential first step for GLP-1 biosynthesis. This proglucagonotropic action of AS1269574 is suppressed by a specific GPR119 antagonist (TM43718) (21), thereby demonstrating that AS1269574 is a potent GPR119 agonist. Unexpectedly, we also find that in STC-1 cells, AS1269574 exerts a novel GPR119-independent action whereby it stimulates the opening of transient receptor potential ankyrin 1 (TRPA1) cation channels (22). This TRPA1 channel activation leads to Ca^{2+} influx and an increase of intracellular free calcium concentration ($[Ca^{2+}]_i$) that triggers the Ca^{2+}-dependent exocytosis of GLP-1. Such findings are significant in view of the recent report that mouse intestinal L cells express not only GPR119 (8) but also TRPA1 channels (23). Thus, new findings presented here indicate that AS1269574 acts as a dual GPR119/TRPA1 agonist to simultaneously up-regulate GLP-1 biosynthesis and release.

Materials and Methods

Cell culture

GLUTag cells were provided by Dr D. J. Drucker (University of Toronto, Toronto, Canada) for culture, as described (7). STC-1 cells and human embryonic kidney-293 (HEK-293) cells were obtained from the American Type Culture Collection. They were grown in DMEM (Thermo Fisher Scientific) containing 25 mM glucose and supplemented with 10% fetal bovine serum and 1% penicillin-streptomycin. All cell cultures were passaged twice a week while kept at 37°C in a humidified incubator gassed with 5% CO_2.

Experimental solutions

The standard extracellular solution (SES) for all experiments contained (in millimoles): 138 NaCl, 5.6 KCl, 2.6 $CaCl_2$, 1.2 $MgCl_2$, 5.6 glucose, and 10 HEPES adjusted to pH 7.4 with NaOH. A Ca^{2+}-free SES was made by isosmotic replacement of $CaCl_2$ with NaCl and 10 μM EGTA. For patch clamp experiments, the TRPA1 cation channel current was measured using a pipette solution containing (in millimoles): 140 Cs-glutamate, 10 NaCl, 1 $MgCl_2$, 0.2 EGTA, 2 MgATP, and 5 HEPES adjusted to pH 7.4 with CsOH.

Measurement of $[Ca^{2+}]_i$

The fura-2 loading solution contained SES supplemented with 0.2% fetal bovine serum, 0.01% Pluronic F-127, and 1 μM fura 2-AM (Thermo Fisher Scientific). Cells were exposed to this solution for 30 minutes at room temperature. Measurements of $[Ca^{2+}]_i$ were performed in a 96-well format at room temperature using a FlexStation 3 plate reader controlled with SoftMax Pro software (Molecular Devices). Excitation light was delivered at either 335/9 nm or 375/9 nm, and the emitted light was detected at 505/15 nm using a 435 nm dichroic mirror. Analysis and plotting of the data were performed using Origin version 8.0 (OriginLab). Results for each time point are presented as data averaged from 12 wells on a single 96-well plate. They are representative of a minimum of three independent experiments. Data are shown using a five-point moving average algorithm. Responses are illustrated as the increase in 335/375 nm fura-2 ratio above baseline. Test solutions were added to individual wells using the automated injection function of the FlexStation 3 at time points indicated by vertical arrows in the figures.

Single-cell measurements of $[Ca^{2+}]_i$ were performed at room temperature using fura-2 loaded cells plated on glass coverslips (Thermo Fisher Scientific; 25 mm, number 1) and mounted on a Nikon Ti inverted microscope equipped with a $\times$40 Super Fluor oil immersion objective (N.A. 1.3). Excitation light of 340 and 380 nm wavelengths was delivered by a DeltaRam monochromator (PTI) via a light guide. The filter set was comprised of a 400-nm long-pass dichroic mirror and a 510/80 nm emission filter (Chroma Technology Corp). Image acquisition was performed using a Cascade II electron-multiplying charge coupled device camera (Photometrics) under the control of Metafluor software (Molecular Devices). Single-cell fura-2 ratios were calculated after subtraction of the background fluorescence that was measured in a cell-free region of the field of view.

Simultaneous detection of endoplasmic reticulum (ER) and cytosolic Ca^{2+}

Ratiometric detection of D1ER and fura-2 fluorescence was performed using methodology similar to that described previously by us (24, 25). Briefly, STC-1 cells were transduced for 16 hours with adenovirus directing expression of the ER-targeted cameleon reporter D1ER (26). Two days later, the cells were

loaded with fura-2 and imaged using a Cascade 650 electron-multiplying charge coupled device camera interfaced with a Nikon TE-2000U inverted microscope. For the D1ER assay that detects fluorescence resonance energy transfer (FRET), we used a 436/10 nm excitation filter in combination with 485/40 and 535/30 nm emission filters. For the fura-2 assay, we used 340/11 and 380/11 nm excitation filters in combination with a 520/11 nm emission filter. For both the D1ER and fura-2 filter sets, we used a 455-nm-long pass dichroic mirror. To perform the simultaneous detection of ER and cytosolic Ca^{2+} in single cells, we used a Lambda 10–2 optical filter changer (Sutter Instruments) so that the light path could be switched quickly between the D1ER and fura-2 filter sets. Ca^{2+} release from the ER leads to a decrease of ER Ca^{2+} content, and this effect is measurable as a decrease of the D1ER 535:485 nm emission ratio. Simultaneously, an increase of the 340:380 nm fura-2 excitation ratio signifies an increase of cytosolic $[Ca^{2+}]_i$ that results from ER Ca^{2+} release. All filter set components were from Chroma Technology Corp.

A-kinase activity reporter 3 (AKAR3) assay

STC-1 cells were transduced for 16 hours with adenovirus directing expression of the FRET reporter AKAR3 (27) using methodology described previously by us (28, 29). Briefly, the culture media were removed and replaced by 170 μL/well of SES containing 11.1 mM glucose and 0.1% BSA so that assays could be performed using a FlexStation 3 microplate reader (Molecular Devices). Excitation light was delivered at 435/9 nm using a 455-nm cutoff dichroic mirror, and emitted light was detected at 485/15 nm (cyan fluorescent protein) or 535/15 nm (yellow fluorescent protein [YFP]). For each well, the average emission intensity was calculated on the basis of 12 excitation flashes for each time point. Test solutions dissolved in SES containing 0.1% dimethylsulfoxide were placed in V-bottom, 96-well plates (Greiner Bio-One), and an automated pipetting procedure was used to transfer 30 μL of each test solution to the assay plate containing cells. The cyan fluorescent protein to YFP emission ratio was calculated for each well, and the values for eight wells were then averaged. The time course of the change of FRET ratio was plotted after exporting these data to Origin version 8.0 (OriginLab).

Patch-clamp assay

Membrane currents were recorded in the tight-seal, whole-cell configuration using bath and pipette solutions described above in the experimental solutions (30). Coverslips on which the cells were adherent were placed in a temperature-controlled perifusion microincubator (model PDMI-2; Harvard Apparatus). Pipettes were pulled from thin-walled glass (catalog number G85150T-4; Warner Instruments) using a Sutter P-97 puller and had resistances of 2–5 MΩ when filled with pipette solution. Measurements of membrane currents were obtained using an EPC-9 amplifier controlled using PatchMaster software (HEKA Electronik). Test solutions were applied to individual cells from a puffer pipette by pneumatic pressure ejection using a Picospritzer III (Parker Hannifin). TRPA1 channel currents were measured at a holding potential of −60 mV, and the current-voltage relationships were obtained by subtracting background currents from activated TRPA1 currents measured during voltage ramps applied at 1 V/sec. Data were digitized and recorded at a sampling frequency of 10 kHz after filtering at 1–3 kHz. The current amplitudes were normalized to whole-cell capacitance.

GLP-1 secretion assay

GLP-1 secretion was measured under conditions of static incubation in which STC-1 cells were incubated in DMEM containing 5.6 mM glucose and 0.1% BSA. Cells were pretreated for 15 minutes with TRPA1 channel blockers prior to administration of AS1269574. For basal and stimulatory conditions, the test intervals were 30 minutes. Secreted GLP-1 was detected using an ELISA kit (EZGLP1T-36K; EMD Millipore) in combination with a Benchmark Plus spectrophotometer and Microplate Manager software (Bio-Rad Laboratories). Each experiment was repeated three times so that the data are the average of three experiments. Data were evaluated for statistical significance by a paired *t* test. A value of $P < .05$ was considered to be statistically significant.

Reverse transcriptase-polymerase chain reaction

RNA was extracted from cells using an RNeasy kit (QIAGEN). RNA concentration was determined using a NanoDrop 2000C spectrophotometer (Thermo Scientific). A QuantiTect SYBR Green one-step reverse transcriptase PCR kit (QIAGEN) was used to generate cDNA per the kit instructions and with control reactions performed without reverse transcriptase. Primers directed against mouse TRPA1 (GenBank NM_177781.4) were designed using Primer3 software (SimGene.com). The forward primer had the nucleic acid sequence (5′-ATGTCACCCCTTCACATAGC-3′), and it was used in combination with a reverse primer (5′-CGTGTTCCCATTCTCTCCTT-3′). For mouse GPR119 (NM_181751.2), the forward primer was 5′-CCAGCCAG-GAATCGTGGTCCAGA-3′, and the reverse primer was 5′AGTCCTGCAGCGTCTTAGCCAT-3′. The cDNA synthesis and PCRs were performed using an MJ Mini thermal cycler (Bio-Rad Laboratories) controlled with CFX Manager software (Bio-Rad Laboratories). Samples containing the reaction mixtures were heated to 50°C for 30 minutes to initiate reverse transcription, after which the samples were held at 95°C for 15 minutes to activate DNA polymerase. A PCR was then performed using 36 cycles of 95°C for 15 seconds, 57°C for 30 seconds, and 72°C for 30 seconds. PCR products with the sizes of 108 bp (TRPA1) and 98 bp (GRPR119) were resolved on 2% agarose gels, and the product identities were confirmed by DNA sequencing using the respective forward primers. RT-PCR for human GPR119 (NM_178471.2) was performed as described (7).

Luciferase reporter assays

The RIP1-CRE-Luc assay was performed as described previously (31). RIP1-CRE-Luc consists of four multimerized nonpalindromic cAMP response elements (CREs) found within the rat insulin 1 gene promoter (RIP1) and that are fused to the coding sequence of firefly luciferase in pLuc-MCS (31). Two days after transfection with this plasmid, cells were exposed for 4 hours to serum-free medium containing 0.1% BSA and the indicated test substances for experimental treatments. Cells were lysed in Passive lysis buffer (Promega), and the lysates were assayed in triplicate for photoemissions using a luciferase assay kit (Promega) and a FlexStation 3 microplate reader (Molecular Devices). Similar protocols (7) were followed using −1100 and −2400 GLU-Luc reporters that contain either −1100 bp or −2400 bp of the rat proglucagon gene promoter fused to luciferase (20). Each experiment was repeated three times so that the data are the average of three experiments. Data were

evaluated for statistical significance by a paired *t* test. A value of $P < .05$ was considered to be statistically significant.

Sources of reagents

AS1269574 was from EMD Millipore. AR231453 was from EnzoLife Scientific. TM43718 was from ChemDiv (compound identification E897-0145). Forskolin, isobutylmethylxanthine (IBMX), oleoylethanolamide (OEA), nimodipine, ω-conotoxin GVIA, ω-agatoxin IVA, and kurtoxin were from Sigma-Aldrich. Diltiazem and cilnidipine were from Santa Cruz Biotechnology Inc. ML218, A967079, AP-18, and HC030031 were from Tocris Biosciences, R&D Systems. Wild-type and C622S rat TRPA1 channel expression plasmids were from Professor E. R. Liman (University of Southern California, Los Angeles, California). Mouse GPR119 cDNA (GenBank NM_181741) in plasmid pCMV6-Entry was from OriGene. Human GPR119 was cloned from human islets of Langerhans, as described previously (7). AKAR3 and D1ER expression plasmids for adenovirus production were provided by Professors. Jin Zhang (Johns Hopkins University School of Medicine, Baltimore, Maryland) and R. Y. Tsien (University of California, San Diego, California). All transient transfections were performed using Lipofectamine and Plus reagent according to the manufacturer's protocol (Life Technologies).

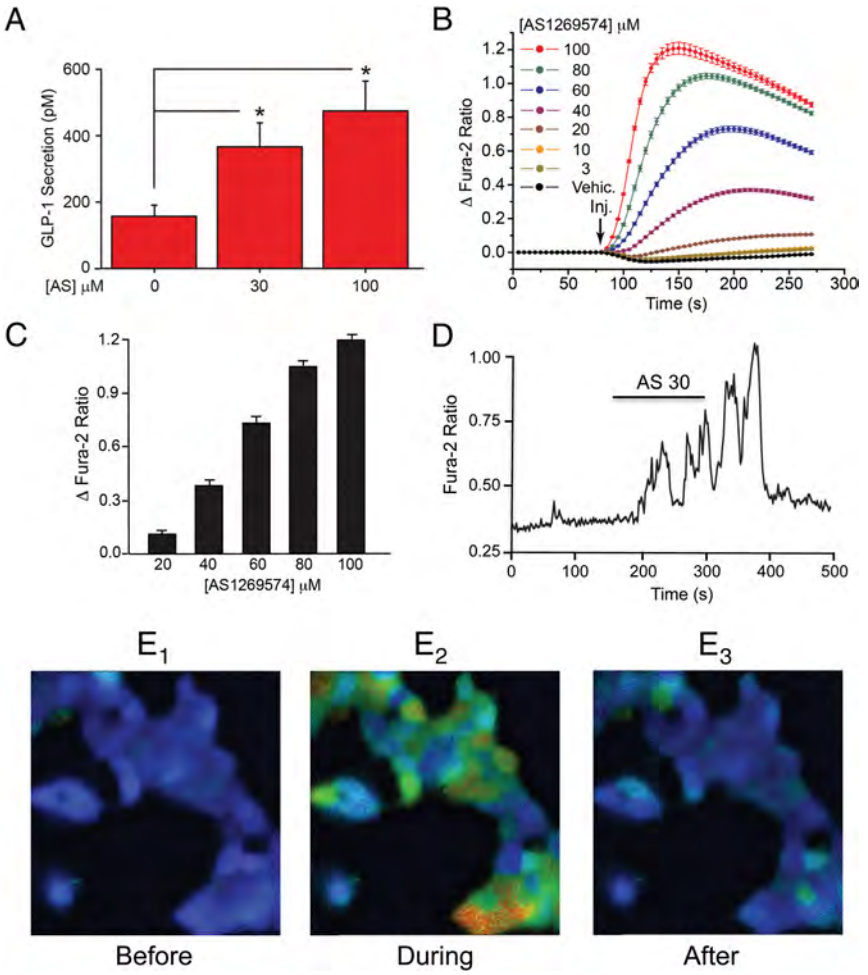

Figure 1. AS1269574 stimulates GLP-1 release and increases $[Ca^{2+}]_i$ in STC-1 cells. A, AS1269574 (AS) exerted a dose-dependent action to stimulate the release of immunoreactive GLP-1 from STC-1 cells in static incubation assays. Data are averaged from five independent assays *, $P < .02$ (paired *t* test; see *Materials and Methods* for experimental details). B, AS1269574 but not the control vehicle solution containing 0.1% dimethylsulfoxide (vehicle) exerted a dose-dependent action to increase $[Ca^{2+}]_i$ in fura-2 loaded STC-1 cell monolayers. A vertical arrow indicates when the test solutions were administered to individual wells of a 96-well plate, here and in all subsequent figures. Concentrations of test substances are the final concentrations present in the individual wells after injection of the test solutions, here and in all subsequent figures. C, The maximal increase of $[Ca^{2+}]_i$ for a range of AS1269574 concentrations, as derived from the raw data presented in panel B. D, AS1269574 (AS; 30 μM) stimulated oscillations of $[Ca^{2+}]_i$ in a single fura-2 loaded STC-1 cell. The horizontal bar indicates the time course during which AS1269574 was administered via a micropipette positioned immediately adjacent to the cell. B–D, For all examples depicted here, the findings are representative of a single experiment that was repeated a minimum of five times on five different occasions with similar results. E_1–E_3, Pseudocolor radiometric images of fura-2 fluorescence in clusters of STC-1 cells in which blue represents a low $[Ca^{2+}]_i$; green-yellow indicates an intermediate $[Ca^{2+}]_i$, and red indicates a high $[Ca^{2+}]_i$. Panels in E_1–E_3 indicate levels of $[Ca^{2+}]_i$ before, during, and after application of AS1269574 (100 μM). These individual images were derived from the accompanying Supplemental Movie.

Results

AS1269574 stimulates GLP-1 release and increases $[Ca^{2+}]_i$ in STC-1 cells

AS1269574 (for structure, see Supplemental Figure 1A) exerted a dose-dependent action to stimulate GLP-1 release from STC-1 cells when it was tested at 30 and 100 μM (Figure 1A). Because GLP-1 release from L cells occurs by Ca^{2+}-dependent exocytosis (32), the potential action of AS1269574 to increase $[Ca^{2+}]_i$ in STC-1 cells was investigated. Fura-2 assays using STC-1 cell monolayers revealed a dose-dependent action of AS1269574 to increase $[Ca^{2+}]_i$ (Figure 1, B and C, and Supplemental Figure 2). This effect of AS1269574 occurred over a concentration range of 20–100 μM, similar to that in which it stimulated GLP-1 release. This action of AS1269574 was rapid in onset and did not fully recover due to the fact that the plate reader assay does not allow washout of test substances. However, by performing single-cell imaging, we found that bath-applied AS1269574 stimulated oscillations of $[Ca^{2+}]_i$ that were terminated after the washout of AS1269574 from the superfusate (Figure 1, D and $E_{1–3}$; see Supplemental Movie).

If GPR119 mediates the action of AS1269574 to increase $[Ca^{2+}]_i$, this action of AS1269574 should be mimicked by other GPR119 agonists not related in structure to AS1269574. Surprisingly, the GPR119 agonists AR231453 (6 μM; see reference 4) and OEA (30 μM; see reference 6) failed to increase $[Ca^{2+}]_i$ when each was tested at a concentration that is known to activate GPR119 (Figure 2A). This outcome was also the case when testing 50 μM AR231453 and 100 μM OEA (data not shown). Furthermore, the action of 30 μM AS1269574 to increase $[Ca^{2+}]_i$ was resistant to 10 μM of the GPR119 antagonist TM43718 (21) (Figure 2B; for structure, see Supplemental Figure 1B). No cross-desensitization between AS1269574 and AR231453 was measurable because pretreatment of STC-1 cells with AR231453 failed to modify the subsequent action of AS1269574 (Figure 2C). Thus, preliminary evidence indicated that AS1269574 exerted a novel GPR119-independent action to increase $[Ca^{2+}]_i$ in STC-1 cells.

Although GPR119 mRNA in STC-1 cells was readily detectable by RT-PCR analysis (see Figure 5C), it might be argued that the level of endogenous GPR119 expression is not sufficiently high and that this limitation explains why certain GPR119 agonists such as AR231453 and OEA are ineffective in assays of $[Ca^{2+}]_i$. If so, AR231453 and OEA might fail to activate a signaling mechanism in which GPR119 stimulation leads to cAMP production with a consequent increase of $[Ca^{2+}]_i$ that results from Ca^{2+} influx and/or intracellular Ca^{2+} release. Such a scenario is unlikely because transfection of STC-1 cells with recombinant mouse GPR119 failed to render these cells capable of responding to AR231453 (6 μM) or OEA (30 μM) in assays of $[Ca^{2+}]_i$ (Supplemental Figure 3).

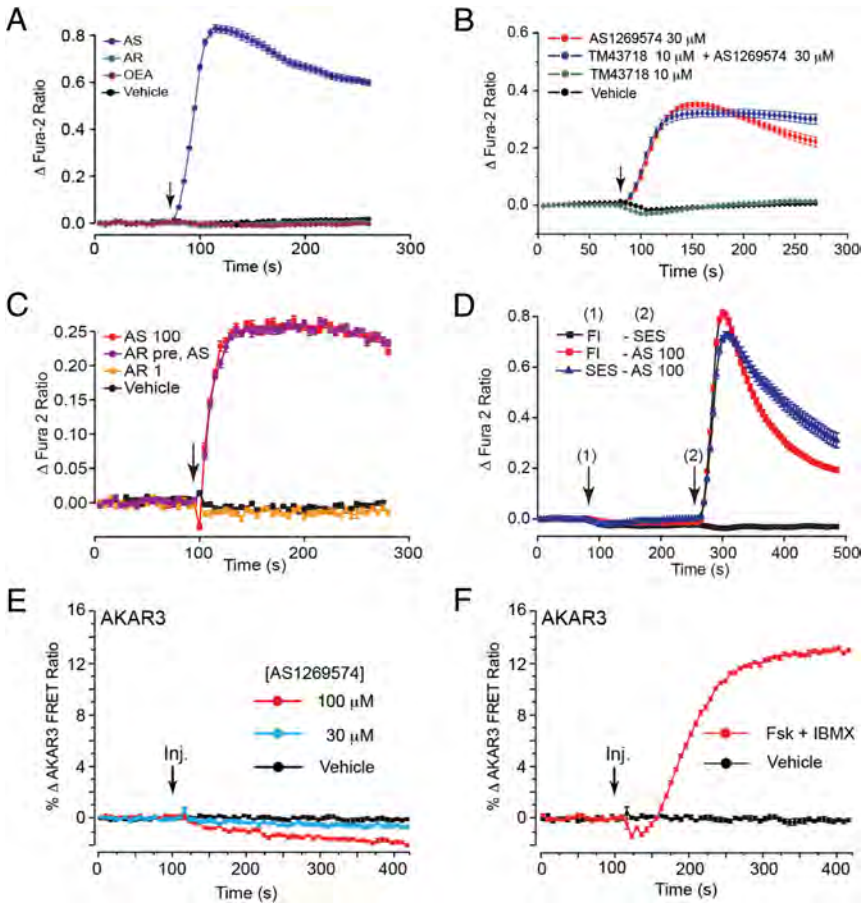

Figure 2. GPR119-independent actions of AS1269574 to increase $[Ca^{2+}]_i$ but not cAMP in STC-1 cell monolayers. A, GPR119 agonists AR231453 (AR; 6 μM), and OEA (30 μM) failed to increase $[Ca^{2+}]_i$, whereas AS1269574 (AS; 100 μM) did so. B, GPR119 antagonist TM43718 failed to significantly alter the action of AS1269574 to increase $[Ca^{2+}]_i$. C, AR231453 (1 μM) failed to increase $[Ca^{2+}]_i$ under standard assay conditions (AR 1), whereas AS1269574 (AS; 100 μM) did so. Pretreatment with AR231453 (1 μM) for 15 minutes (AR pre, AS) failed to alter the subsequent action of AS1269574 (100 μM). D, A two-step injection mode assay revealed that combined administration of forskolin (F; 2 μM) and IBMX (I; 100 μM) failed to increase $[Ca^{2+}]_i$ (FI, arrow 1, black trace), nor did the SES vehicle solution have any subsequent effect (SES, arrow 2, black trace). In the absence of forskolin, an initial injection of SES vehicle solution was without effect (SES, arrow 1, blue trace), whereas AS1269574 (100 μM) stimulated an increase of $[Ca^{2+}]_i$ (AS 100, arrow 2, blue trace). When forskolin and IBMX were administered together during the initial injection (FI, arrow 1, red trace), there was no increase of $[Ca^{2+}]_i$, and the subsequent action of AS1269574 (AS 100, arrow 2, red trace) was not modified. E and F, AS1269574 (30 or 100 μM) failed to raise levels of cAMP, as inferred from its failure to induce an increase of the 535:484 nm AKAR3 FRET ratio (E). However, an increase of the 534:484 nm AKAR3 FRET ratio was measured in response to the positive control test solution containing forskolin (Fsk; 2 μM) and IBMX (100 μM). A–F, For all examples depicted here, the findings are representative of a single experiment that was repeated a minimum of three times on three different occasions with similar results.

AS1269574 acts independently of cAMP production to increase $[Ca^{2+}]_i$

The cAMP-elevating agents forskolin and IBMX failed to raise levels of $[Ca^{2+}]_i$ in STC-1 cells (Figure 2D), thereby indicating that cAMP is unlikely to mediate a stimulatory action of AS1269574 on $[Ca^{2+}]_i$. Furthermore, forskolin and IBMX failed to modify the action of AS1269574 (Figure 2D). To more directly test for an acute stimulatory effect of AS1269574 on cAMP production, STC-1 cell monolayers were virally transduced with a genetically encoded AKAR3 that exhibits an increase of 535:485 nm FRET emission ratio when it is phosphorylated by cAMP-dependent protein kinase (protein kinase A

[PKA)] (27). In this AKAR3 assay, AS1269574 had no immediate ability to increased the 535:485 nm FRET ratio despite the fact that forskolin and IBMX were effective (Figure 2, E and F). Nevertheless, to evaluate a potential long-term action of AS1269574 to stimulate cAMP production, STC-1 cell monolayers were transfected with a RIP1-CRE-Luc luciferase reporter that is responsive to cAMP-elevating agents such as forskolin and IBMX (31). In this assay, RIP1-CRE-Luc activity was not significantly stimulated after a 4-hour exposure of STC-1 cells to AS1269574 (see Supplemental Figure 8A). Collectively these findings indicated that AS1269574 did not activate a conventional GPR119 signaling pathway that is coupled to cAMP production in STC-1 cells.

AS1269574 promotes Ca^{2+} influx in STC-1 cells

AS1269574 (30 or 100 μM) failed to stimulate an increase of $[Ca^{2+}]_i$ under conditions in which STC-1 cells were equilibrated in a nominally Ca^{2+}-free solution (Figure 3A and Supplemental Figure 4). This finding indicated that AS1269574 raised levels of $[Ca^{2+}]_i$ by promoting Ca^{2+} influx. Because STC-1 cells are electrically excitable (33–35), Ca^{2+} influx stimulated by AS1269574 might be explained by entry of Ca^{2+} through voltage-dependent Ca^{2+} channels (VDCCs) (36). Alternatively, AS1269574 might promote Ca^{2+} entry through nonselective cation channels (NSCCs) (37). To distinguish between these two different mechanisms of Ca^{2+} entry, we tested Ca^{2+} channel blockers that are selective for L, N, P/Q, and T subtypes of VDCCs (36). None of these blockers significantly inhibited the action of AS1269574 to increase $[Ca^{2+}]_i$ (Supplemental Figure 5). However, trivalent (La^{3+}) and divalent (Ni^{2+}) cations that block both VDCCs and NSCCs (37) did exert an inhibitory effect (Supplemental Figure 6, A–C).

Interestingly, an apparent increase of $[Ca^{2+}]_i$ was measured in response to the divalent cation Cd^{2+} (Supplemental Figure 6D). This finding is significant because the TRPA1 channel subtype of NSCC is activated by Cd^{2+} (38). Having noted the prior report of Emery et al (23) that the TRPA1 channel activator allyl isothiocyanate (AITC) stimulated GLP-1 release from L-cell cultures of wild-type but not *Trpa1* knockout mice, we then established that 100 μM AS1269574 failed to stimulate an increase of $[Ca^{2+}]_i$ under conditions in which STC-1 cells were treated with 300 nM of the selective TRPA1 channel blocker A967079 (39) (Figure 3B). This finding indicated that functional TRPA1 channels are expressed in STC-1 cells, and it is consistent with our RT-PCR detection of TPRA1 channel mRNA in STC-1 cells (see Figure 5C) and also the previously published data of Emery et al (23). Thus, preliminary target validation was achieved indicating that AS1269574 exerted novel TRPA1 channel-activating properties in STC-1 cells.

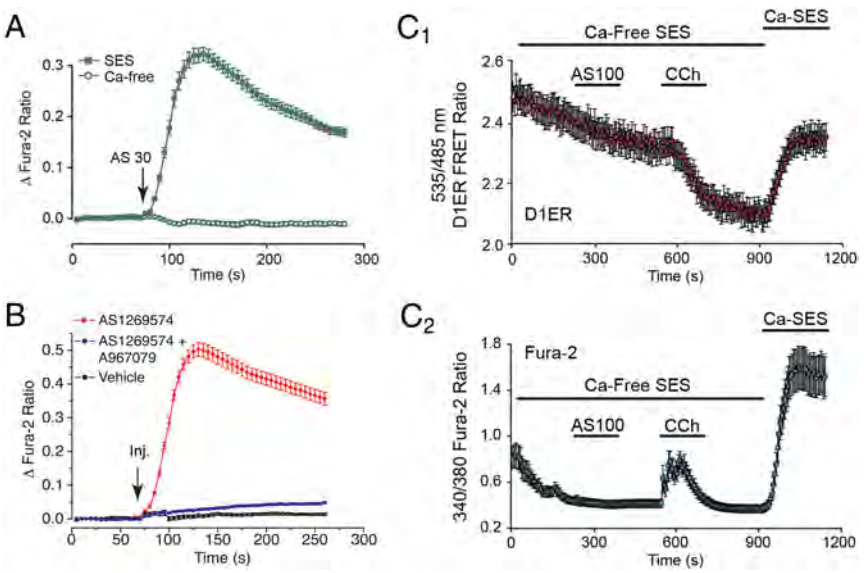

Figure 3. AS1269574 promotes Ca^{2+} influx but not ER Ca^{+} mobilization in STC-1 cells. A, AS1269574 (AS; 30 μM) failed to increase $[Ca^{2+}]_i$ in STC-1 cell monolayers when the SES was nominally Ca^{2+} free (Ca-free). B, The action of AS1269574 (AS; 100 μM) to increase $[Ca^{2+}]_i$ was nearly eliminated under conditions in which STC-1 cells were pretreated for 15 minutes with 300 nM of the TRPA1 blocker A967079 and then coadministered 100 μM AS1269574 in combination with 300 nM A967079. C1 + C2, the actions of 100 μM AS1269574 (AS; 100) and 250 μM carbachol (CCh) were evaluated in STC-1 cells expressing a D1ER Ca^{2+} biosensor targeted to the ER (C_1), and also loaded with fura-2 so that the cytosolic $[Ca^{2+}]$ could be simultaneously monitored (C_2). Experiments were initiated using a nominally Ca^{2+}-free extracellular solution (Ca-Free SES) after which the normal extracellular solution containing Ca^{2+} was reintroduced (Ca-SES). Carbachol but not AS1269574 released Ca^{2+} from the ER, as inferred from the decrease of D1ER 535:485 nm FRET ratio (C_1). An accompanying increase of cytosolic Ca^{2+} was measured in the same cell in response to carbachol but not AS1269574 (C_2). A–C, For all examples depicted here, the findings are representative of a single experiment that was repeated a minimum of three times on three different occasions with similar results.

AS1269574 fails to mobilize ER Ca^{2+} in STC-1 cells

When considering a TRPA1 channel-mediated action of AS1269574 to increase $[Ca^{2+}]_i$, the potential role of intracellularly released Ca^{2+} must be taken into account due to the fact that cytosolic Ca^{2+} can activate TRPA1 channels (40, 41). Therefore, STC-1 cells

were transduced with the ER-targeted Ca^{2+} reporter D1ER (26) so that any Ca^{2+} mobilizing action of AS1269574 could be monitored (Figure $3C_1$). Simultaneously, cells were loaded with fura-2 so that any ER Ca^{2+} release could be detected as an increase of cytosolic $[Ca^{2+}]_i$ (Figure $3C_2$). For these live-cell imaging assays, a decrease of D1ER 535:485 nm emission ratio signifies a decrease of ER $[Ca^{2+}]_i$, whereas an increase of the 340/380 nm fura-2 ratio signifies an increase of cytosolic $[Ca^{2+}]_i$. By imaging the fluorescent properties of these two reporters in single STC-1 cells, it was possible to demonstrate that AS1269574 failed to mobilize Ca^{2+}, whereas the positive control cholinergic agonist carbachol was effective (Figure 3, C_1 and C_2).

TRPA1 channel activation by AITC, carvacrol, and AS1269574 in STC-1 cells

Consistent with the previously reported expression of TRPA1 channels in STC-1 cells (23, 42–47), the naturally occurring TRPA1 channel activators AITC (48) and carvacrol (49) exerted dose-dependent actions to increase $[Ca^{2+}]_i$ in STC-1 cells (Figure 4, A and B). We then established that the selective TRPA1 channel blockers A967079 and HC030031 (50) dose dependently inhibited the increase of $[Ca^{2+}]_i$ measured in response to AS1269574 (Figure 4, C and D). Using patch-clamp analysis of STC-1 cells loaded with fura-2, it was also possible to demonstrate that brief focal application of AS1269574 to a single cell led to the generation of a transient inward membrane current and a simultaneous increase of $[Ca^{2+}]_i$ under conditions of voltage clamp (Figure 5, A_1 and A_2). The time courses of these two responses were nearly identical, as expected if Ca^{2+} influx through TRPA1 channels was responsible for the increase of $[Ca^{2+}]_i$. The current-voltage (I-V) relationship for the membrane current activated by AS1269574 exhibited outward rectification (Figure 5B), as reported for various *Trp* channels including TRPA1 (41).

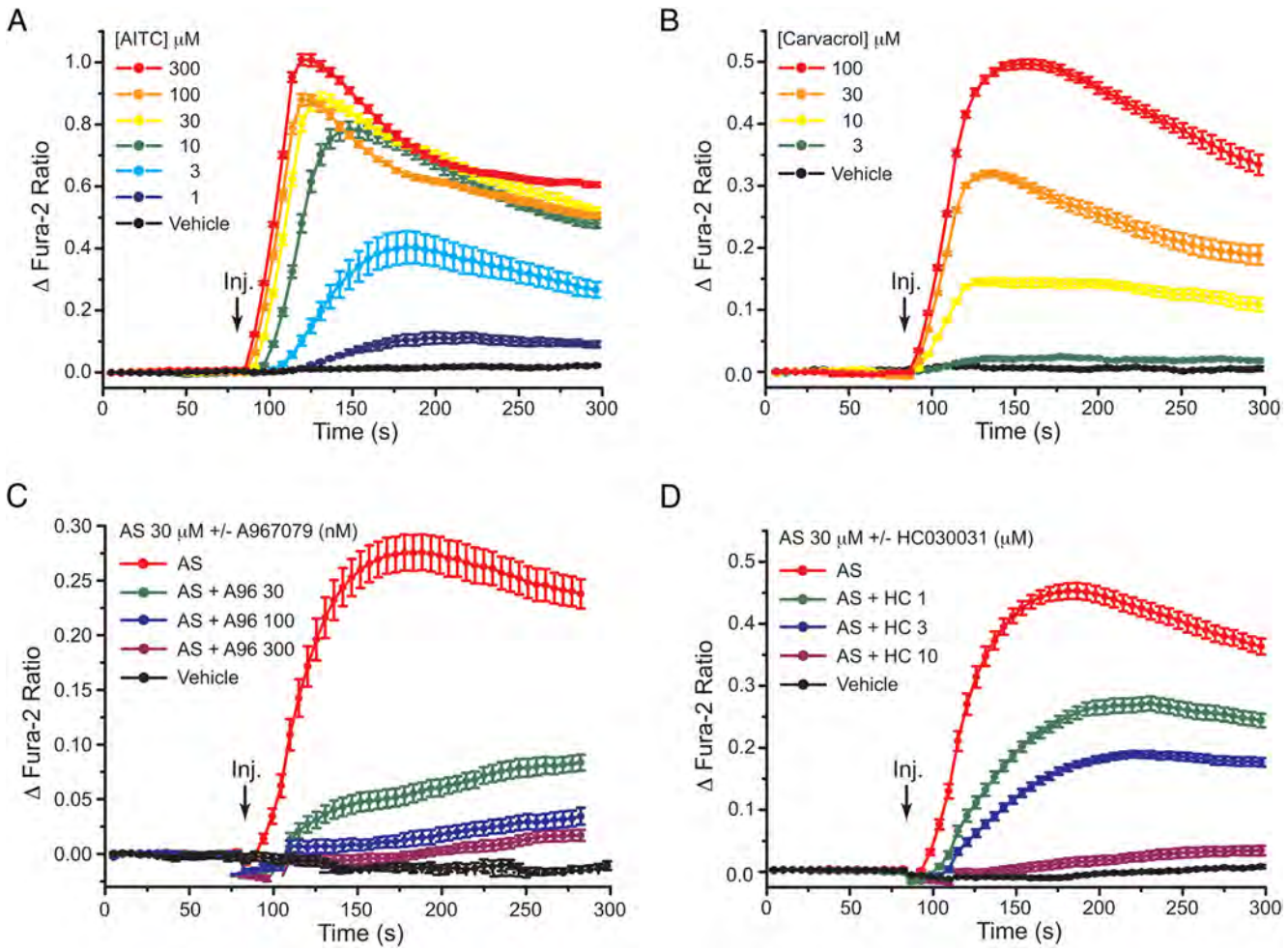

Figure 4. TRPA1 channel activation by AITC, carvacrol, and AS1269574 in STC-1 cells. A, Dose-dependent action of 1–300 μM AITC to raise $[Ca^{2+}]_i$. B, Dose-dependent action of 3–100 μM carvacrol to raise $[Ca^{2+}]_i$. C, Dose-dependent action of A967079 (A96; 30, 100, or 300 nM) to block TRPA1 channel activation by 30 μM AS1269574 (AS). D, Dose-dependent action of HC030031 (HC; 1, 3, or 10 μM) to block TRPA1 channel activation by 30 μM AS1269574 (AS). A–D, For all examples depicted here, the findings are representative of a single experiment that was repeated a minimum of three times on three different occasions with similar results.

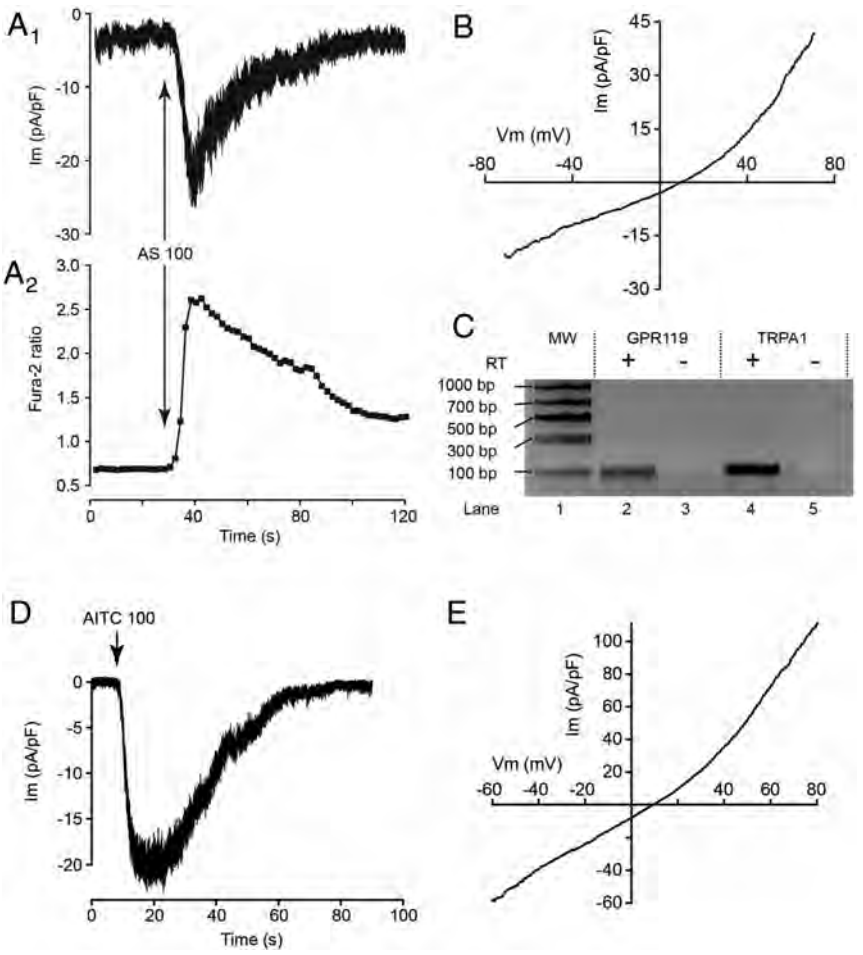

Figure 5. AS1269574 and AITC activate inward currents to increase $[Ca^{2+}]_i$ in STC-1 cells. A, AS1269574 (AS 100) was applied at a concentration of 100 μM for 5 seconds directly to a single STC-1 cell (vertical arrows). The experiment was performed under conditions of whole-cell voltage clamp (−60 mV pipette holding potential) in which the cell was loaded with fura-2. AS1269574 activated an inward membrane current (A_1), the time course of which closely matched the accompanying increase of $[Ca^{2+}]_i$ (A_2) in the same cell. Nearly identical findings were obtained in three separate experiments using a total of 10 cells. B, To determine the I-V relationship of the membrane current activated by AS1269574, the pipette potential was shifted as a voltage ramp from −70 mV to +70 mV (1 Vs^{-1}). The baseline ramp current measured in the absence of AS1269574 was subtracted from the ramp current measured in the presence of AS1269574 so that the difference current could be calculated. The difference current is plotted as a function of the pipette potential in order to obtain the I-V relationship that indicates outward rectification characteristic of TRPA1 channels. For the illustrated cell, the reversal potential for the ramp current was +9 mV. For a total of 12 cells studied, the mean value of the reversal potential was +4 ± 2 mV (n = 12). C, RT-PCR detection of GPR119 and TRPA1 mRNA in STC-1 cells (reverse transcriptase [RT]). D, Representative example of the membrane current activated by a 5-second application of AITC (100 μM) to an STC-1 cell using methods described for panel A, above. Nearly identical findings were obtained in two separate experiments using a total of eight cells. E, Representative example of the I-V relationship for the membrane current activated by AITC. Note the close correspondence of this I-V relationship to that of panel B for AS1269574. For the illustrated cell, the reversal potential for the ramp current was +10 mV. For a total of 12 cells studied, the mean value of the reversal potential was +11 ± 2 mV (n = 12).

Consistent with the expression of TRPA1 channel mRNA in STC-1 cells (Figure 5C), the TRPA1 channel activator AITC also induced an inward current with an outwardly rectifying I-V relationship (Figure 5, D and E). As noted above, this was also the case for the membrane current activated by AS1269574 (Figure 5B). By performing fura-2 assays at the single-cell level, it was established that individual STC-1 cells consistently responded to both AS1269574 and AITC (Figure 6, A–D). In summary, such findings provided additional evidence that AS1269574 activated TRPA1 channels in STC-1 cells. As discussed below, further target validation was achieved by demonstrating an ability of AS1269574 to activate recombinant rat TRPA1 channels expressed in HEK-293 cells.

GLP-1 secretion stimulated by AS1269574 requires TRPA1 channel activation

Emery et al (23) demonstrated that GLP-1 secretion from mouse L-cell cultures was stimulated by the TRPA1 channel activators AITC and carvacrol and that these actions of AITC and carvacrol were fully inhibited by the TRPA1 channel blocker HC030031. However, no reports presently exist concerning investigational GLP-1 secretagogues that are TRPA1 channel activators. Here we hypothesized that the TRPA1 channel activation by AS1269574 in STC-1 cells generates Ca^{2+} influx so that the consequent increase of $[Ca^{2+}]_i$ initiates exocytosis of GLP-1. Consistent with this prediction, the GLP-1 secretagogue action of AS1269574 was inhibited by multiple TRPA1 channel blockers in static incubation assays of STC-1 cell monolayers (Figure 7). Thus, when AS1269574 was tested at a concentration of either 30 or 100 μM, its ability to stimulate GLP-1 release was strongly suppressed by the TRPA1 channel blockers A967079, HC030031, and AP-18 (51). Interestingly, basal GLP-1 release measured in the absence of AS1269574 was unaffected by TRPA1 blockers. This finding is expected if basal TRPA1 channel activity in STC-1 cells is especially low under the experimental conditions described here.

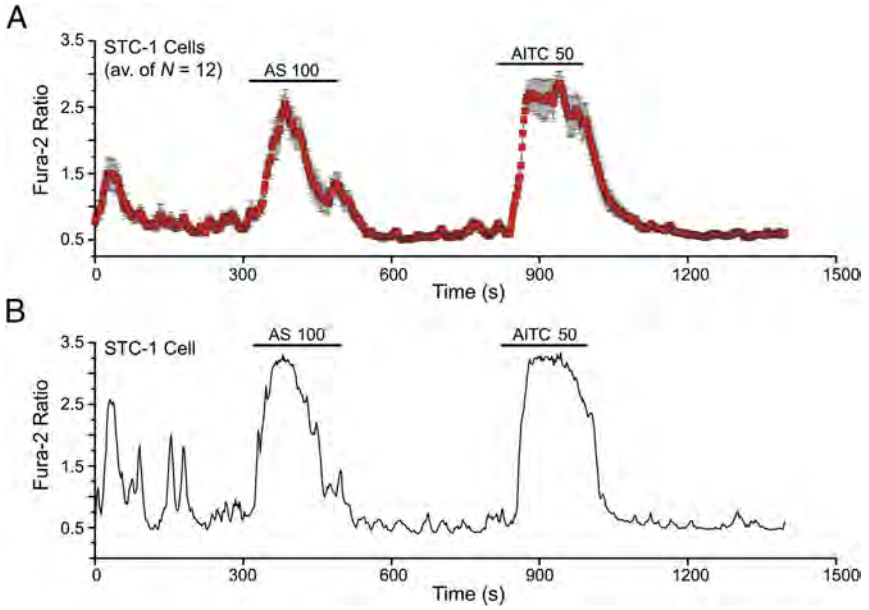

Figure 6. Coexistence of AS1269574 and AITC sensitivity in STC-1 cells. A, A population study of 12 fura-2 loaded STC-1 cells on a single coverslip demonstrated that these cells responded to sequential administration of 100 μM AS1269574 (AS 100) and 50 μM AITC (AITC 50). B, A representative example of a cell described in panel A in which AS1269574 and AITC both stimulated an increase of $[Ca^{2+}]_i$. A and B, The findings are representative of a single experiment using 12 cells for panel A, and 10 cells for panel B. Each experiment was repeated a minimum of three times on three different occasions with similar results.

AS1269574 activates recombinant TRPA1 channels in transfected HEK-293 cells

AS1269574 and AITC were also tested in patch-clamp studies using HEK-293 cells transfected with wild-type (WT) rat TRPA1 cDNA (rTRPA1) or an empty vector (EV) that served as a negative control. For this analysis, rTRPA1 was fused at its N terminus to YFP so that single cells expressing rTRPA1 could be positively identified on the basis of their YFP fluorescence (52). AS1269574 and AITC both induced a transient inward current under conditions of voltage clamp in cells transfected with rTRPA1 (Figure 8, A and C). However, no responses were measureable in cells transfected with the EV (n = 10 cells, data not shown). These currents activated by AS1269574 and AITC exhibited outward rectification (Figure 8, B and D), similar to that that was observed for the currents activated by AS1269574 and AITC in STC-1 cells (Figure 5, B and E). Because HEK-293 cells do not express endogenous GPR119 (53, 54), the simplest explanation for these findings is that AS1269574 directly activated rTRPA1 channels. Therefore, target validation was achieved in that we demonstrated a GPR119-independent action of AS1269574 to activate rat TRPA1 channels.

AS1269574 activates recombinant TRPA1 channels to increase $[Ca^{2+}]_i$ in HEK-293 cells

Surprisingly, for HEK-293 cells transfected with the EV, a modest increase of $[Ca^{2+}]_i$ was measured in response to AS1269574 (Figure 9A). However, this increase of $[Ca^{2+}]_i$ did not result from TRPA1 channel activation because it was not reduced by the TRPA1 channel blocker A967079 (Figure 9A). Instead, this increase of $[Ca^{2+}]_i$ resulted from intracellular Ca^{2+} mobilization because it was measured under Ca^{2+}-free conditions (Supplemental Figure 7, A and B). Note that for HEK-293 cells expressing WT rTRPA1 channels, a considerably larger increase of $[Ca^{2+}]_i$ was measured in response to AS1269574 (Figure 9B). This additional increase of $[Ca^{2+}]_i$ resulted from TRPA1 channel-mediated Ca^{2+} influx because it was inhibited by extracellular Ni^{2+} (Supplemental Figure 7, and D) or by treatment with A967079 (Figure 9B). Collectively such findings provided additional evidence that AS1269574 directly activates TRPA1 channels.

AS1269574 activates mutant C622S TRPA1 channels in HEK-293 cells

TRPA1 channel activators can be divided into two broad categories: electrophilic and nonelectrophilic agonists (55, 56). Channel activity is stimulated by electrophilic agonists such as AITC that covalently modify conserved Cys and Lys residues located near the channel's N terminus (55, 56). Cys>Ser substitutions at these residues reduce the ability of electrophiles to activate the channel. However, such mutations have little impact on channel activity stimulated by nonelectrophiles such as carvacrol (55, 56). Consistent with a nonelectrophilic mechanism of channel activation, AS1269574 stimulated an increase $[Ca^{2+}]_i$, and the magnitude of this effect was nearly identical for HEK-293 cells transfected with WT rTRPA1 or a mutant C622S rTRPA that has a reduced sensitivity to electrophiles (57) (cf, Figure 9, C and D). In contrast, the increase of $[Ca^{2+}]_i$ measured in response to the electrophile AITC was reduced in HEK-293 cells expressing C622S rTRPA1 as compared with WT rTRPA1 (cf, Figure 9, E and F). What still remains to be determined is whether AS1269574 has any capacity to act as an electrophile at Cys residues other than C622. This is unlikely because the chemical structure of AS1269574 is not indicative of it being an electrophile (personal communication with J Wu, PhD, Dartmouth College, Hanover, New Hampshire).

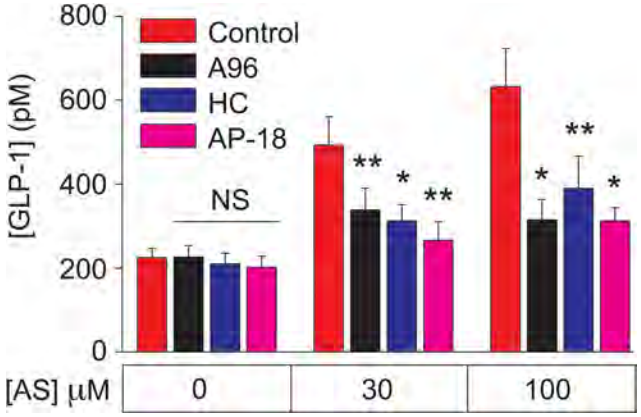

Figure 7. STC-1 cell GLP-1 release stimulated by AS1269574 requires TRPA1 channel activation. The action of AS1269574 (AS, 30 or 100 μM) to stimulate GLP-1 release from STC-1 cells was inhibited by the TRPA1 channel blockers A967079 (A96; 1 μM), HC030031 (HC; 10 μM), and AP-18 (15 μM). *, $P < .03$, **, $P < .01$ (paired *t* test). NS, not significant. These data are the average of three independent experiments (see *Materials and Methods*).

Cell type-specific actions of AS1269574 to control proglucagon gene expression

Although AS1269574 exerted novel TRPA1 channel-activating properties in STC-1 cells, it remained possible that this compound might activate GPR119 to control other cellular functions. Therefore, to test for GPR119 agonist action, CRE-based reporter gene expression assays were performed using cell lines that express: 1) endogenous mouse GPR119 (STC-1, GLUTag), or 2) HEK-293 cells that do not express endogenous GPR119 or 3) HEK-293 cells that were transfected with recombinant human GPR119. For such assays, each cell line was transfected with the RIP1-CRE-Luc reporter (31) or −1100- and −2400-bp GLU-Luc reporters that incorporate the CREs from the proglucagon gene promoter (20). These GLU-Luc reporters were previously used by us to demonstrate that AS1269574 stimulates proglucagon gene promoter activity in GLUTag cells (7).

For STC-1 cells that express GPR119, the RIP1-CRE-Luc and −2400 GLU-Luc reporters were relatively insensitive to AS1269574 when compared with forskolin and IBMX (Supplemental Figure 8, A and B). Similar findings were obtained using the −1100 GLU-Luc reporter (data not shown). These results are surprising in view of the previously reported action of AS1269574 to stimulate CRE-Luc activity in HEK-293 cells transfected with human GPR119 (12). However, such results are consistent with our finding that AS1269574 failed to stimulate cAMP production in STC-1 cells, as evaluated using the AKAR3 FRET reporter (see Figure 2, E and F). With these unexpected findings in mind, we evaluated whether AS1269574 would stimulate RIP1-CRE-Luc activity in HEK-293 cells transfected with recombinant human GPR119. No such stimulatory effect was measureable despite the fact that the GPR119 agonist AR231453 was effective (Supplemental Figure 9, C and D). Thus, contrary to one prior report (12), AS1269574 had little or no ability to stimulate CRE-based reporters that are cAMP regulated.

Despite these negative findings for STC-1 and HEK-293 cells, low concentrations (0.3–3.0 μM) of AS1269574-stimulated −1100 GLU-Luc activity in GLUTag cells (Figure 10, A and B). This was also the case for GLUTag cells expressing the −2400 GLU-Luc reporter (Figure 10C). Note that the stimulatory effect of AS1269574 was detected in GLUTag cells transfected with a control empty vector (Figure 10A) or mouse GPR119 (Figure 10B). Also note that for GLUTag cells transfected with mouse GPR119, the stimulatory action of AS1269574 (Figure 10B) was superimposed on the in-

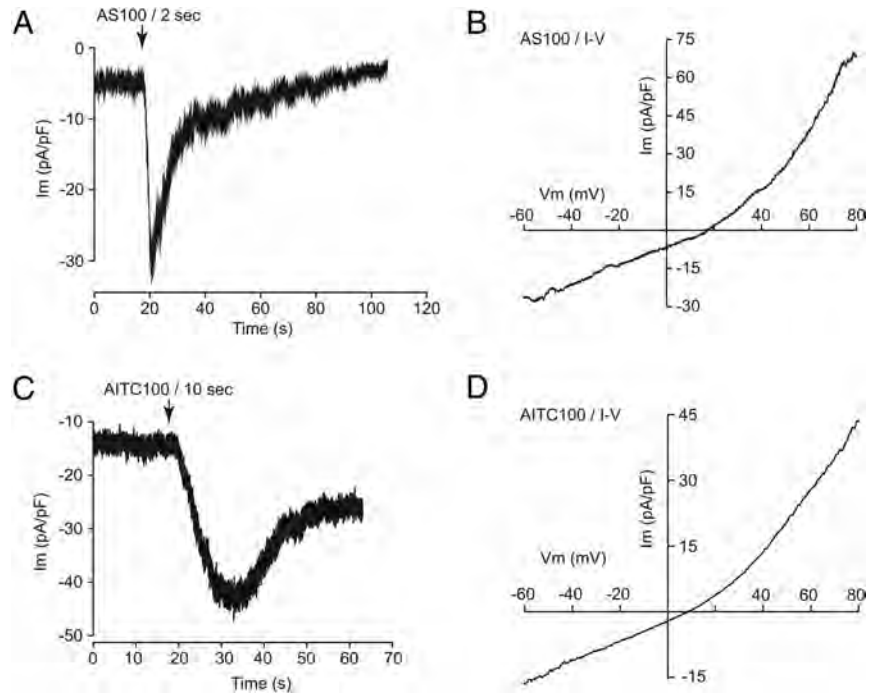

Figure 8. AS1269574 and AITC activate rat TRPA1 channels in HEK-293 cells. A and B, Inward current (A; mean amplitude −22 ± 5 pA/PF; n = 16 cells; −60 mV holding potential) and I-V relationship (B; mean reversal potential +15 ± 2 mV; n = 6 cells) for HEK-293 cells transfected with rat TRPA1 and exposed to 100 μM AS1269574 (AS 100) for 2 seconds. C and D, Inward current (C; mean amplitude −19 ± 3 pA/PF; n = 12 cells; −60 mV holding potential) and I-V relationship (D; mean reversal potential +10 ± 4 mV; n = 7 cells) for HEK-293 cells transfected with rat TRPA1 and exposed to 100 μM AITC (AS 100) for 10 seconds.

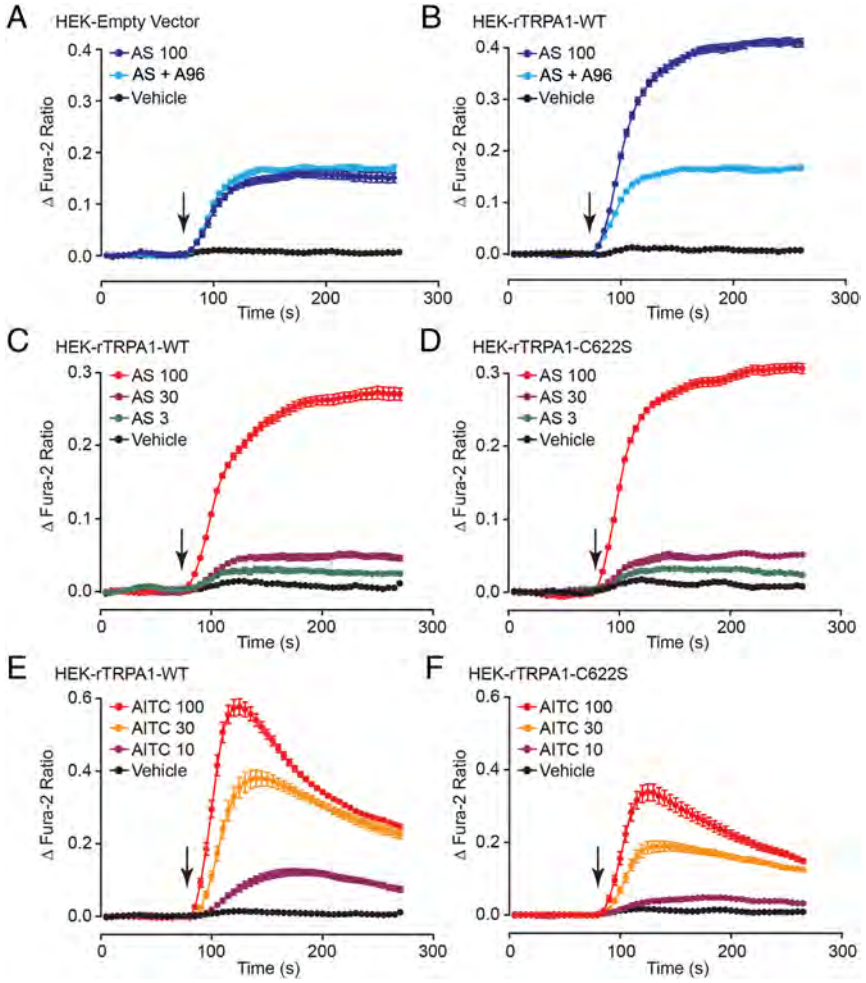

Figure 9. AS1269574 activates recombinant rat TRPA1 channels to increase $[Ca^{2+}]_i$ in HEK-293 cells. A and B, Comparison of the actions of AS1269574 (AS; 100 μM) to increase $[Ca^{2+}]_i$ in HEK-293 cells transfected with a control EV (A) or WT rTRPA1 16 hours after the transfection (B). Note that the TRPA1 channel blocker A967079 (A96; 0.3 μM) exerted no effect in cells transfected with the EV, whereas it suppressed the incremental increase of $[Ca^{2+}]_i$ stimulated by AS1269574 in cells transfected with WT rTRPA1. Although not illustrated, for cells transfected with EV or rTRPA1, the baseline fura-2 ratio values at the start of the assay (10 sec time point) corresponded to 1.02 ± 0.03 and 1.07 ± 0.02, respectively. Thus, basal levels of $[Ca^{2+}]_i$ were not significantly increased in cells transfected with rTRPA1. C and D, Comparison of the actions of AS1269574 (AS; 3, 30, or 100 μM) to increase $[Ca^{2+}]_i$ in HEK-293 cells transfected with WT (C) or mutant C622S (D) rTRPA1 channel plasmid DNA. The action of AS1269574 was unaffected by introduction of the C > S amino acid substitution. E and F, Comparison of the actions of AITC (10, 30, or 100 μM) to increase $[Ca^{2+}]_i$ in HEK-293 cells transfected with WT (C) or mutant C622S (D) rTRPA1 channel plasmid DNA. The action of AITC was reduced by introduction of the C > S amino acid substitution. A–F, For all examples depicted here, the findings are representative of a single experiment that was repeated a minimum of three times on three different occasions with similar results.

crease of basal GLU-Luc activity that resulted from the previously reported constitutive and ligand-independent action of recombinant GPR119 to increase basal −1100 GLU-Luc activity (7). Remarkably, the GPR119 antagonist TM43718 abrogated all such stimulatory actions of AS1269574 in these assays of −1100 GLU-Luc activity (Figure 10, A and B). Thus, AS1269574 activated endogenous GPR119 in GLUTag cells to stimulate proglucagon gene promoter activity. Collectively these findings established the cell type-specific nature with which AS1269574 exerted a proglucagonotropic action. Nevertheless, it remained uncertain whether this action of AS1269574 was mediated by a conventional GPR119 and cAMP signaling mechanism.

AS1269574 stimulates GLU-Luc activity independently of cAMP and PKA

We previously reported a constitutive and ligand-independent action of recombinant GPR119 to stimulate GLU-Luc activity in transfected GLUTag cells (7). This constitutive action of GPR119 was shown to be mediated by PKA and not by the cAMP-regulated guanine nucleotide exchange factor designated as Epac2 (7). Furthermore, GLU-Luc activity was unaffected by a cAMP analog that is a selective activator of Epac2, whereas a selective activator of PKA did produce a stimulatory effect (7). What is presently uncertain is whether agonist binding to endogenous GPR119 recapitulates the constitutive and ligand-independent action of recombinant GPR119 to stimulate GLU-Luc in a PKA-dependent manner. For example, GPR119 was reported to be coexpressed in L cells with the heterotrimeric G protein α-gustducin that can signal independently of cAMP and that stimulates GLP-1 release (8, 58), Thus, it was of interest to determine whether in GLUTag cells, AS1269574 stimulated GLU-Luc activity in a PKA dependent or independent manner.

Consistent with the already established ability of cAMP-elevating agents to activate PKA and to stimulate proglucagon gene expression in GLUTag cells (16), forskolin and IBMX stimulated −2400 GLU-Luc activity under control conditions, but failed to do so under conditions in which GLUTag cells were treated with the PKA inhibitor H-89 (Figure 10D). Although H-89 also reduced the stimulatory action of AS1269574 at −2400 GLU-Luc, the magnitude of this inhibition was especially small (Figure 10E). Thus, a role for cAMP as a signaling molecule important

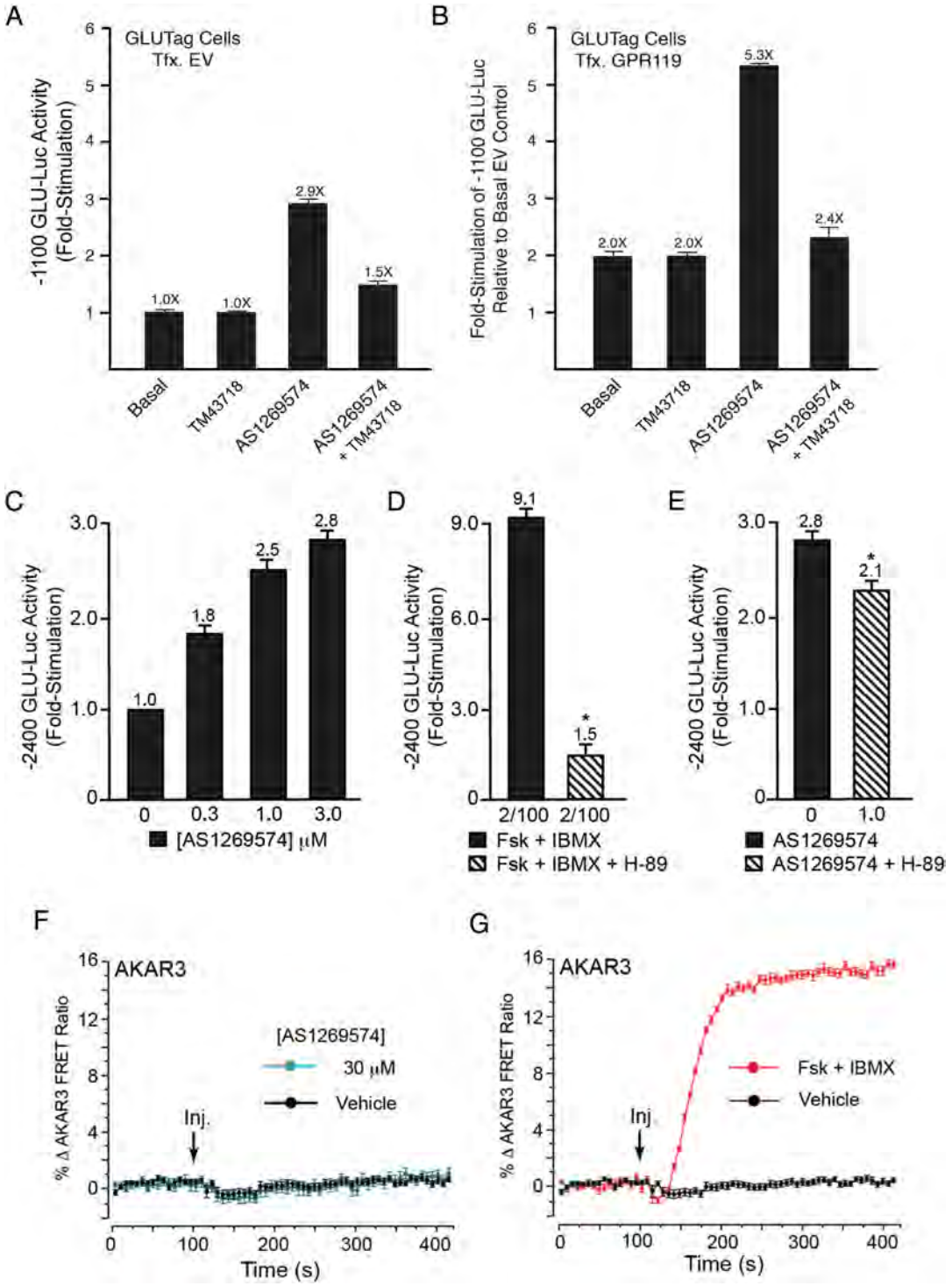

Figure 10. GPR119 antagonist TM43718 suppresses PKA-independent stimulation of proglucagon gene promoter activity by AS1269574 in GLUTag cells. A and B, TM43718 (10 μM) and AS1269574 (10 μM) were administered alone, or in combination, so that their abilities to alter −1100 bp GLU-Luc activity could be determined for GLUTag cells transfected with EV or mouse GPR119. For both experimental conditions, the stimulatory action of AS1269574 was suppressed by TM43718. Due to the constitutive ligand-independent activity of GPR119, the basal activity of −1100 bp GLU-Luc was elevated in cells transfected with GPR119. Therefore, data in panels A and B are depicted such that a fold-stimulation value of 1 corresponds to basal luciferase activity measured for cells transfected with EV. C, Dose-response relationship for the stimulatory effect of AS1269574 at −2400 GLU-Luc. Note that AS1269574 exerts its effect at concentrations 10 times lower than that measured in assays of $[Ca^{2+}]_i$. D and E, The serine/threonine protein kinase inhibitor H-89 (10 μM) nearly abolished the actions of forskolin (2 μM) and IBMX (100 μM) to stimulate −2400 GLU-Luc (D), whereas a much smaller inhibitory effect was measured when testing AS1269574 (E). F and G, AS1269574 (30 or 100 μM) failed to raise levels of cAMP (F), whereas forskolin (2 μM) and IBMX (100 μM) did so (G), as measured in GLUTag cells virally transduced with AKAR3. A–G, For all examples depicted here, the findings are representative of a single experiment that was repeated a minimum of three times on three different occasions with similar results.

to the action of AS1269574 was drawn into question. By imaging GLUTag cells transduced with AKAR3, it was then established that AS1269574 failed to raise levels of cAMP in this cell type (Figure 10F), whereas forskolin and IBMX did so (Figure 10G). Remarkably, AS1269574 also failed to stimulate RIP1-CRE-Luc activity in GLUTag cells (Supplemental Figure 9). Taken as a whole, such findings indicated that binding of AS1269574 to GPR119 did not recapitulate the constitutive and ligand-independent action of GPR119 to signal through PKA to stimulate proglucagon gene expression.

Discussion

Unexpected TRPA1 channel-activating properties of AS1269574

New findings reported here demonstrate that AS1269574 has the surprising ability to act as a TRPA1 channel agonist so that it has the capacity to increase $[Ca^{2+}]_i$ and to stimulate the release of GLP-1 from STC-1 cells. These actions of AS1269574 are independent of GPR119 activation and are not secondary to Ca^{2+} mobilization or the stimulation of cAMP production. Instead, AS1269574 directly promotes Ca^{2+} influx through TRPA1 channels so that the ensuing increase of $[Ca^{2+}]_i$ stimulates GLP-1 exocytosis. Target validation that AS1269574 activates TRPA1 channels is obtained in studies of HEK-293 cells expressing recombinant rat TRPA1. What remains to be determined is whether AS1269574 acts independently of covalent channel modification to gate TRPA1 channels from a closed to open conformation. This might be the case because a mutant C622S TRPA1 channel that has reduced sensitivity to electrophiles is fully responsive to AS1269574.

The ability of AS1269574 to increase $[Ca^{2+}]_i$ and to stimulate GLP-1 release from STC-1 cells is suppressed by the selective TRPA1 channel blockers A967079, AP-18, and HC030031. However, GPR119 agonists such AR231453 and OEA do not replicate the action of AS1269574 to increase $[Ca^{2+}]_i$ in STC-1 cells, nor is the Ca^{2+}-elevating action of AS1269574 inhibited by a selective GPR119 antagonist (TM43718). Thus, TRPA1 channel activation by AS1269574 is established to be GPR119 independent. Because AS1269574 is the prototype of a series of 2,4,6 trisubstituted pyrimidines that are reported for preclinical studies of GPR119 agonist action (10, 11), it will be important to take into account off-target effects of AS1269574 to activate TRPA1 channels that are reported to be expressed in L cells and pancreatic β-cells that secrete GLP-1 and insulin, respectively (23, 59). For example, TRPA1 channel activation might contribute to the ability of AS1269574 to stimulate insulin secretion from mouse islets (60). Thus, the TRPA1 channel-mediated action of AS1269574 established here adds a new dimension to the interpretation of prior studies documenting improved glucoregulation in mice administered 2,4,6 trisubstituted pyrimidines such as AS1269574 (12–15).

Dual agonist properties of AS1269574

Although AS1269574 directly activates TRPA1 channels in STC-1 cells, we find that AS1269574 also acts in a GPR119-dependent manner to stimulate proglucagon gene expression in GLUTag cells. This GPR119-dependent action of AS1269574 is fully inhibited by the GPR119 antagonist TM43718. Remarkably, such findings indicate that AS1269574 has dual GPR119/TRPA1 agonist properties that might be of high significance when evaluating how it improves systemic glucose homeostasis in vivo. Thus, AS1269574 acts via GPR119 to stimulate proglucagon gene expression so that L-cell GLP-1 biosynthesis is up-regulated. Simultaneously, AS1269574 acts independently of GPR119 to directly promote TRPA1 channel activation and Ca^{2+} influx that initiates GLP-1 secretion. Potentially it might be possible to achieve selective activation of GPR119 when using an appropriate dosing regimen because GPR119 and TRPA1 channel activation occur at low and high doses of AS1269574, respectively.

Cell type-specific actions of AS1269574

Findings reported here are the first to document the cell type-specific action of AS1269574 to up-regulate proglucagon gene expression. Thus, we find that AS1269574 exerts a stronger effect to stimulate GLU-Luc reporter activity in GLUTag cells as compared with STC-1 cells. Because AS1269574 fails to stimulate cAMP production in both GLUTag cells and STC-1 cells, this cell type-specific action of AS1269574 is not explained by differential expression of a signaling pathway that couples GPR119 to G_s proteins, adenylyl cyclase, and cAMP production. Instead, the cell type-specific action of AS1269574 might be explained by differential coupling of GPR119 to the G protein α-gustducin that is expressed at high levels in GLUTag cells but at low levels in STC-1 cells (58). Importantly, GPR119 and α-gustducin are coexpressed in the intestinal L cells (8) and α-gustducin is implicated in the control of GLP-1 release (8). Thus, a rationale exists for future studies that will explore the putative role of α-gustducin in the control of GLP-1 biosynthesis by GPR119 agonists such as AS1269574.

Targeting TRPA1 channels to identify new GLP-1 secretagogues

TRPA1 channels continue to be studied from the standpoint of their established roles in peripheral sensory neuron function in which they participate in the sensations of pain, cold, and itch (22, 61, 62). TRPA1 is one member of a larger family of *Trp* channels, many of which are also expressed in the gastrointestinal tract (63, 64). Using methods of cell sorting to obtain select populations of intestinal enteroendocrine cells, Emery et al (23) recently reported that TRPA1 is expressed in mouse L cells. Because TRPA1 channels are activated by pungent compounds commonly found in food (mustard oil, cinnamon oil, wintergreen oil, ginger), TRPA1 channels might participate in the sensing of nutrients by intestinal L cells so that GLP-1 secretion is stimulated after a meal. If so, the possibility exists that L-cell function might be stimulated by small molecule drugs that target TRPA1 channels. Thus, TRPA1 activators might find an unexpected role in therapeutics as a new class of GLP-1 secretagogues.

Although controversy exists concerning whether L-cell GLP-1 secretion is defective in patients with T2DM (65), it seems possible that a beneficial blood glucose-lowering effect might be achieved after oral administration of a small molecule TRPA1 channel activator to these patients. In fact, the dietary TRPA1 channel activator cinnamaldehyde exerts blood glucose-lowering and weight-reducing actions in mice (66). However, therapeutic targeting of L cells might be challenging if orally administered TRPA1 channel activators exert additional effects at TRPA1 channels expressed on other types of cells within the gastrointestinal tract (eg, enterochromaffin cells that express TRPA1 channels and that secrete serotonin to stimulate gastric motility) (67). Furthermore, it is not yet clear what added benefit a GLP-1 secretagogue would have in comparison with available GLP-1 receptor agonists or dipeptidyl peptidase-4 inhibitors (68, 69). Finally, potential actions of TRPA1 channel agonists to generate pain by activating visceral nociceptive sensory neurons must be taken into account (61, 62). However, it is worth noting that TRPA1 channel activators are commonly found in food and that they are well tolerated. Thus, it makes sense to expand drug discovery efforts to include the identification of novel GLP-1 secretagogues with TRPA1 channel-activating properties.

Conclusion

The two principal outcomes of the present study are as follows: 1) the discovery of unexpected TRPA1 channel-activating properties of AS1269574 and 2) the demonstration that TRPA1 channel activation is essential for AS1269574 to stimulate GLP-1 secretion from STC-1 cells. Additional offshoots of this study are the findings that 3) AS1269574 exerts cell type-specific actions to stimulate proglucagon gene expression in a GPR119-mediated manner, and 4) AS1269574 acts as a dual agonist at two molecular targets (GPR119, TRPA1) already established to be of importance to L-cell function. It is especially interesting that proglucagon gene promoter activity in GLUTag cells is stimulated by AS1269574 in a PKA-independent manner, whereas recombinant GPR119 exerts a PKA-dependent stimulatory effect that is both constitutive and ligand independent. Thus, binding of AS1269574 to GPR119 may bias the signaling properties of this receptor so that PKA-independent stimulation of proglucagon gene expression is achieved. In summary, the herein reported dual agonist properties of AS1269574 at GPR119 and TRPA1 channels suggest a new paradigm for drug discovery efforts whereby simultaneous activation of a G protein-coupled receptor and an ion channel is achieved.

Acknowledgments

Address all correspondence and requests for reprints to: Colin A. Leech, PhD, Associate Professor of Medicine, State University of New York Upstate Medical University, IHP 4304 at 505 Irving Avenue, Syracuse, NY, 13210. E-mail: leechc@upstate.edu.

Author contributions include the following: O.G.C. performed the GLP-1 secretion assays and the fura-2, AKAR3, luciferase, and RT-PCR assays. C.A.L. performed the RT-PCR, single-cell fura-2, D1ER, and patch clamp electrophysiology assays. M.W.R. established the fura-2 and D1ER assays for the assessment of the intracellular Ca^{2+} handling. C.A.L., O.G.C., and G.G.H. designed the experiments and wrote the manuscript. G.G.H. conceived the project.

This work was supported by an award from the National Institutes of Health (National Institute of Diabetes and Digestive and Kidney Diseases Grant R01-DK069575 to G.G.H.) and by Basic Science Awards from the American Diabetes Association (Grant 7-12-BS-077 to G.G.H. and Grant 1-12-BS-109 to C.A.L.). Additional support was provided by an award from the National Institutes of Health (National Institute of Diabetes and Digestive and Kidney Diseases Grant R01-DK092616 to M.W.R.).

Disclosure Summary: The authors have nothing disclose.

References

1. **Gamble JM, Clarke A, Myers KJ, et al.** Incretin-based medications for type 2 diabetes: an overview of reviews. *Diabetes Obes Metab*. 2015;17:649–658.
2. **Trujillo JM, Nuffer W, Ellis SL.** GLP-1 receptor agonists: a review

of head-to-head clinical studies. *Ther Adv Endocrinol Metab*. 2015; 6:19–28.
3. **Scheen AJ.** Safety of dipeptidyl peptidase-4 inhibitors for treating type 2 diabetes. *Expert Opin Drug Saf*. 2015;14:505–524.
4. **Semple G, Fioravanti B, Pereira G, et al.** Discovery of the first potent and orally efficacious agonist of the orphan G-protein coupled receptor 119. *J Med Chem*. 2008;51:5172–5175.
5. **Chu ZL, Carroll C, Alfonso J, et al.** A role for intestinal endocrine cell-expressed G protein-coupled receptor 119 in glycemic control by enhancing glucagon-like peptide-1 and glucose-dependent insulinotropic peptide release. *Endocrinology*. 2008;149:2038–2047.
6. **Overton HA, Fyfe MC, Reynet C.** GPR119, a novel G protein-coupled receptor target for the treatment of type 2 diabetes and obesity. *Br J Pharmacol*. 2008;153(suppl 1):S76–S81.
7. **Chepurny OG, Bertinetti D, Diskar M, et al.** Stimulation of proglucagon gene expression by human GPR119 in enteroendocrine L-cell line GLUTag. *Mol Endocrinol*. 2013;27:1267–1282.
8. **Li Y, Kokrashvili Z, Mosinger B, Margolskee RF.** Gustducin couples fatty acid receptors to GLP-1 release in colon. *Am J Physiol Endocrinol Metab*. 2013;304:E651–E660.
9. **Ritter K, Buning C, Halland N, Poverlein C, Schwink L.** G protein-coupled receptor 119 (GPR119) agonists for the treatment of diabetes: recent progress and prevailing challenges. *J Med Chem*. In press.
10. **Negoro K, Yonetoku Y, Misawa-Mukai H, et al.** Discovery and biological evaluation of novel 4-amino-2-phenylpyrimidine derivatives as potent and orally active GPR119 agonists. *Bioorg Med Chem*. 2012;20:5235–5246.
11. **Negoro K, Yonetoku Y, Moritomo A, et al.** Synthesis and structure-activity relationship of fused-pyrimidine derivatives as a series of novel GPR119 agonists. *Bioorg Med Chem*. 2012;20:6442–6451.
12. **Yoshida S, Ohishi T, Matsui T, Shibasaki M.** Identification of a novel GPR119 agonist, AS1269574, with in vitro and in vivo glucose-stimulated insulin secretion. *Biochem Biophys Res Commun*. 2010;400:437–441.
13. **Yoshida S, Ohishi T, Matsui T, et al.** Novel GPR119 agonist AS1535907 contributes to first-phase insulin secretion in rat perfused pancreas and diabetic db/db mice. *Biochem Biophys Res Commun*. 2010;402:280–285.
14. **Yoshida S, Ohishi T, Matsui T, et al.** The role of small molecule GPR119 agonist, AS1535907, in glucose-stimulated insulin secretion and pancreatic β-cell function. *Diabetes Obes Metab*. 2011; 13:34–41.
15. **Yoshida S, Tanaka H, Oshima H, et al.** AS1907417, a novel GPR119 agonist, as an insulinotropic and β-cell preservative agent for the treatment of type 2 diabetes. *Biochem Biophys Res Commun*. 2010;400:745–751.
16. **Drucker DJ, Jin T, Asa SL, Young TA, Brubaker PL.** Activation of proglucagon gene transcription by protein kinase A in a novel mouse enteroendocrine cell line. *Mol Endocrinol*. 1994;8:1646–1655.
17. **Abello J, Ye F, Bosshard A, Bernard C, Cuber JC, Chayvialle JA.** Stimulation of glucagon-like peptide-1 secretion by muscarinic agonist in a murine intestinal endocrine cell line. *Endocrinology*. 1994;134:2011–2017.
18. **Grant SG, Seidman I, Hanahan D, Bautch VL.** Early invasiveness characterizes metastatic carcinoid tumors in transgenic mice. *Cancer Res*. 1991;51:4917–4923.
19. **Rindi G, Grant SG, Yiangou Y, et al.** Development of neuroendocrine tumors in the gastrointestinal tract of transgenic mice. Heterogeneity of hormone expression. *Am J Pathol*. 1990;136:1349–1363.
20. **Jin T, Drucker DJ.** Activation of proglucagon gene transcription through a novel promoter element by the caudal-related homeodomain protein cdx-2/3. *Mol Cell Biol*. 1996;16:19–28.
21. **Engelstoft MS, Norn C, Hauge M, et al.** Structural basis for constitutive activity and agonist-induced activation of the enteroendocrine fat sensor GPR119. *Br J Pharmacol*. 2014;171:5774–5789.
22. **Nilius B, Appendino G, Owsianik G.** The transient receptor potential channel TRPA1: from gene to pathophysiology. *Pflugers Arch*. 2012;464:425–458.
23. **Emery EC, Diakogiannaki E, Gentry C, et al.** Stimulation of GLP-1 secretion downstream of the ligand-gated ion channel TRPA1. *Diabetes*. 2015;64:1202–1210.
24. **Landa LR Jr, Harbeck M, Kaihara K, et al.** Interplay of Ca^{2+} and cAMP signaling in the insulin-secreting MIN6 β-cell line. *J Biol Chem*. 2005;280:31294–31302.
25. **Harbeck MC, Chepurny OG, Nikolaev VO, Lohse MJ, Holz GG, Roe MW.** Simultaneous optical measurements of cytosolic Ca^{2+} and cAMP in single cells. *Sci STKE*. 2006;2006(353):pl6.
26. **Palmer AE, Jin C, Reed JC, Tsien RY.** Bcl-2-mediated alterations in endoplasmic reticulum Ca2+ analyzed with an improved genetically encoded fluorescent sensor. *Proc Natl Acad Sci USA*. 2004; 101(50):17404–17409.
27. **Allen MD, Zhang J.** Subcellular dynamics of protein kinase A activity visualized by FRET-based reporters. *Biochem Biophys Res Commun*. 2006;348:716–721.
28. **Holz GG, Leech CA, Roe MW, Chepurny OG.** High-throughput FRET assays for fast time-resolved detection of cyclic AMP in pancreatic β cells. In: Cheng X, ed. *Cyclic Nucleotide Signaling*. Boca Raton, FL: CRC Press; 2014:35–60.
29. **Schwede F, Chepurny OG, Kaufholz M, et al.** Rp-cAMPS prodrugs reveal the cAMP dependence of first-phase glucose-stimulated insulin secretion. *Mol Endocrinol*. 2015;29:988–1005.
30. **Leech CA, Holz GG 4th.** Application of patch clamp methods to the study of calcium currents and calcium channels. *Methods Cell Biol*. 1994;40:135–151.
31. **Chepurny OG, Holz GG.** A novel cyclic adenosine monophosphate responsive luciferase reporter incorporating a nonpalindromic cyclic adenosine monophosphate response element provides optimal performance for use in G protein coupled receptor drug discovery efforts. *J Biomol Screen*. 2007;12:740–746.
32. **Tolhurst G, Reimann F, Gribble FM.** Nutritional regulation of glucagon-like peptide-1 secretion. *J Physiol*. 2009;587:27–32.
33. **Eiki J, Saeki K, Nagano N, et al.** A selective small molecule glucagon-like peptide-1 secretagogue acting via depolarization-coupled Ca^{2+} influx. *J Endocrinol*. 2009;201:361–367.
34. **Mangel AW, Scott L, Liddle RA.** Depolarization-stimulated cholecystokinin secretion is mediated by L-type calcium channels in STC-1 cells. *Am J Physiol*. 1996;270:G287–G290.
35. **Mangel AW, Snow ND, Misukonis MA, et al.** Calcium-dependent regulation of cholecystokinin secretion and potassium currents in STC-1 cells. *Am J Physiol*. 1993;264:G1031–G1036.
36. **Catterall WA.** Voltage-gated calcium channels. *Cold Spring Harb Perspect Biol*. 2011;3(8):a003947.
37. **Sieman, D.** Nonselective cation channels. In: Siemen D, Hescheler J, eds. *Nonselective Cation Channels: Pharmacology, Physiology, and Biophysics*. Vol 66 of Experientia Supplementum. Basel, Switzerland: Birkhäuser; 1993:3–25.
38. **Miura S, Takahashi K, Imagawa T, Uchida K, Saito S, Tominaga M, Ohta T.** Involvement of TRPA1 activation in acute pain induced by cadmium in mice. *Mol Pain*. 2013;9:7.
39. **Chen J, Joshi SK, DiDomenico S, et al.** Selective blockade of TRPA1 channel attenuates pathological pain without altering noxious cold sensation or body temperature regulation. *Pain*. 2011;152(5): 1165–1172.
40. **Doerner JF, Gisselmann G, Hatt H, Wetzel CH.** Transient receptor potential channel A1 is directly gated by calcium ions. *J Biol Chem*. 2007;282(18):13180–13189.
41. **Zurborg S, Yurgionas B, Jira JA, Caspani O, Heppenstall PA.** Direct activation of the ion channel TRPA1 by Ca^{2+}. *Nat Neurosci*. 2007;10(3):277–279.
42. **Purhonen AK, Louhivuori LM, Kiehne K, Kerman KE, Herzig KH.**

TRPA1 channel activation induces cholecystokinin release via extracellular calcium. *FEBS Lett*. 2008;582:229–232.
43. **Motter AL, Ahern GP.** TRPA1 is a polyunsaturated fatty acid sensor in mammals. *PLoS One*. 2012;7(6):e38439.
44. **McClenaghan C, Zeng F, Verkuyl JM.** TRPA1 agonist activity of probenecid desensitizes channel responses: consequences for screening. *Assay Drug Dev Technol*. 2012;10(6):533–541.
45. **Kurogi M, Miyashita M, Emoto Y, Kubo Y, Saitoh O.** Green tea polyphenol epigallocatechin gallate activates TRPA1 in an intestinal enteroendocrine cell line, STC-1. *Chem Senses*. 2012;37(2):167–177.
46. **Kim HY, Park M, Kim K, Lee YM, Rhyu MR.** Hesperetin stimulates cholecystokinin secretion in enteroendocrine STC-1 cells. *Biomol Ther (Seoul)*. 2013;21(2):121–125.
47. **Nakajima S, Hira T, Yahagi A, et al.** Unsaturated aldehydes induce CCK secretion via TRPA1 in STC-1 cells. *Mol Nutr Food Res*. 2014;58(5):1042–1051.
48. **Bandell M, Story GM, Hwang SW, et al.** Noxious cold ion channel TRPA1 is activated by pungent compounds and bradykinin. *Neuron*. 2004;41(6):849–857.
49. **Xu H, Delling M, Jun JC, Clapham DE.** Oregano, thyme and clove-derived flavors and skin sensitizers activate specific TRP channels. *Nat Neurosci*. 2006;9(5):628–635.
50. **McNamara CR, Mandel-Brehm J, Bautista DM, et al.** TRPA1 mediates formalin-induced pain. *Proc Natl Acad Sci USA*. 2007;104(33):13525–13530.
51. **Petrus M, Peier AM, Bandell M, et al.** A role of TRPA1 in mechanical hyperalgesia is revealed by pharmacological inhibition. *Mol Pain*. 2007;3:40.
52. **Wang YY, Chang RB, Waters HN, McKemy DD, Liman ER.** The nociceptor ion channel TRPA1 is potentiated and inactivated by permeating calcium ions. *J Biol Chem*. 2008;283(47):32691–32703.
53. **Atwood BK, Lopez J, Wager-Miller J, Mackie K, Straiker A.** Expression of G protein-coupled receptors and related proteins in HEK293, AtT20, BV2, and N18 cell lines as revealed by microarray analysis. *BMC Genomics*. 2011;12:14.
54. **Zhang SY, Li J, Xie X.** Discovery and characterization of novel small molecule agonists of G protein-coupled receptor 119. *Acta Pharmacol Sin*. 2014;35(4):540–548.
55. **Hinman A, Chuang HH, Bautista DM, Julius D.** TRP channel activation by reversible covalent modification. *Proc Natl Acad Sci USA*. 2006;103:19564–19568.
56. **Macpherson LJ, Dubin AE, Evans MJ, et al.** Noxious compounds activate TRPA1 ion channels through covalent modification of cysteines. *Nature*. 2007;445:541–545.
57. **Wang YY, Chang RB, Allgood SD, Silver WL, Liman ER.** A TRPA1-dependent mechanism for the pungent sensation of weak acids. *J Gen Physiol*. 2011;137:493–505.
58. **Margolskee RF, Dyer J, Kokrashvili Z, et al.** T1R3 and gustducin in gut sense sugars to regulate expression of Na^+-glucose cotransporter 1. *Proc Natl Acad Sci USA*. 2007;104(38):15075–15080.
59. **Cao DS, Zhong L, Hsieh TH, et al.** Expression of transient receptor potential ankyrin 1 (TRPA1) and its role in insulin release from rat pancreatic β cells. *PLoS One*. 2012;7:e38005.
60. **Moran BM, Abdel-Wahab YH, Flatt PR, McKillop AM.** Activation of GPR119 by fatty acid agonists augments insulin release from clonal β-cells and isolated pancreatic islets and improves glucose tolerance in mice. *Biol Chem*. 2014;395:453–464.
61. **Bautista DM, Jordt SE, Nikai T, et al.** TRPA1 mediates the inflammatory actions of environmental irritants and proalgesic agents. *Cell*. 2006;124:1269–1282.
62. **Mickle AD, Shepherd AJ, Mohapatra DP.** Sensory TRP channels: the key transducers of nociception and pain. *Prog Mol Biol Transl Sci*. 2015;131:73–118.
63. **Boesmans W, Owsianik G, Tack J, Voets T, Vanden Berghe P.** TRP channels in neurogastroenterology: opportunities for therapeutic intervention. *Br J Pharmacol*. 2011;162:18–37.
64. **Fernandes ES, Fernandes MA, Keeble JE.** The functions of TRPA1 and TRPV1: moving away from sensory nerves. *Br J Pharmacol*. 2012;166:510–521.
65. **Faerch K, Torekov SS, Vistisen D, et al.** GLP-1 response to oral glucose is reduced in prediabetes, screen-detected type 2 diabetes, and obesity and influenced by sex: the ADDITION-PRO study. *Diabetes*. 2015;64:2513–2525.
66. **Camacho S, Michlig S, de Senarclens-Bezencon C, et al.** Anti-obesity and anti-hyperglycemic effects of cinnamaldehyde via altered ghrelin secretion and functional impact on food intake and gastric emptying. *Sci Rep*. 2015;5:7919.
67. **Nozawa K, Kawabata-Shoda E, Doihara H, et al.** TRPA1 regulates gastrointestinal motility through serotonin release from enterochromaffin cells. *Proc Natl Acad Sci USA*. 2009;106:3408–3413.
68. **Holz GG, Chepurny OG.** Glucagon-like peptide-1 synthetic analogs: new therapeutic agents for use in the treatment of diabetes mellitus. *Curr Med Chem*. 2003;10:2471–2483.
69. **Nadkarni P, Chepurny OG, Holz GG.** Regulation of glucose homeostasis by GLP-1. *Prog Mol Biol Transl Sci*. 2014;121:23–65.

Supplemental Fig.S1

A

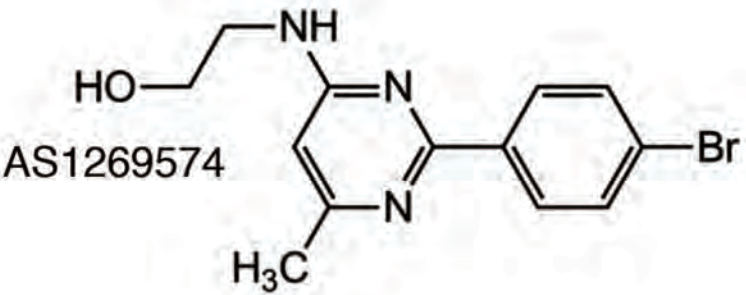

B

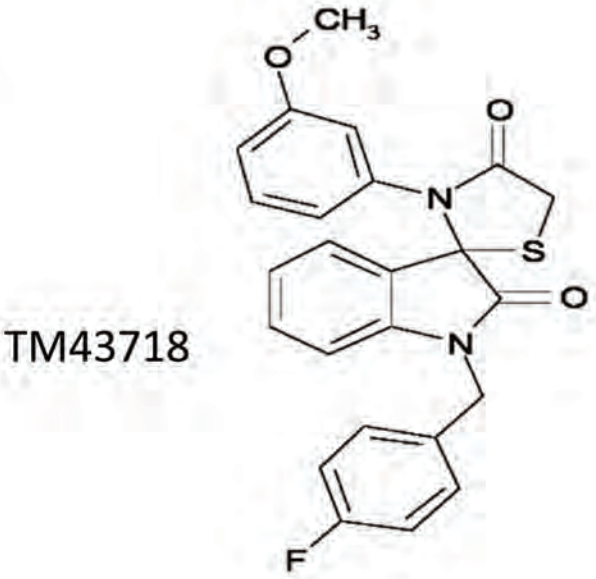

Supplemental Fig.S2

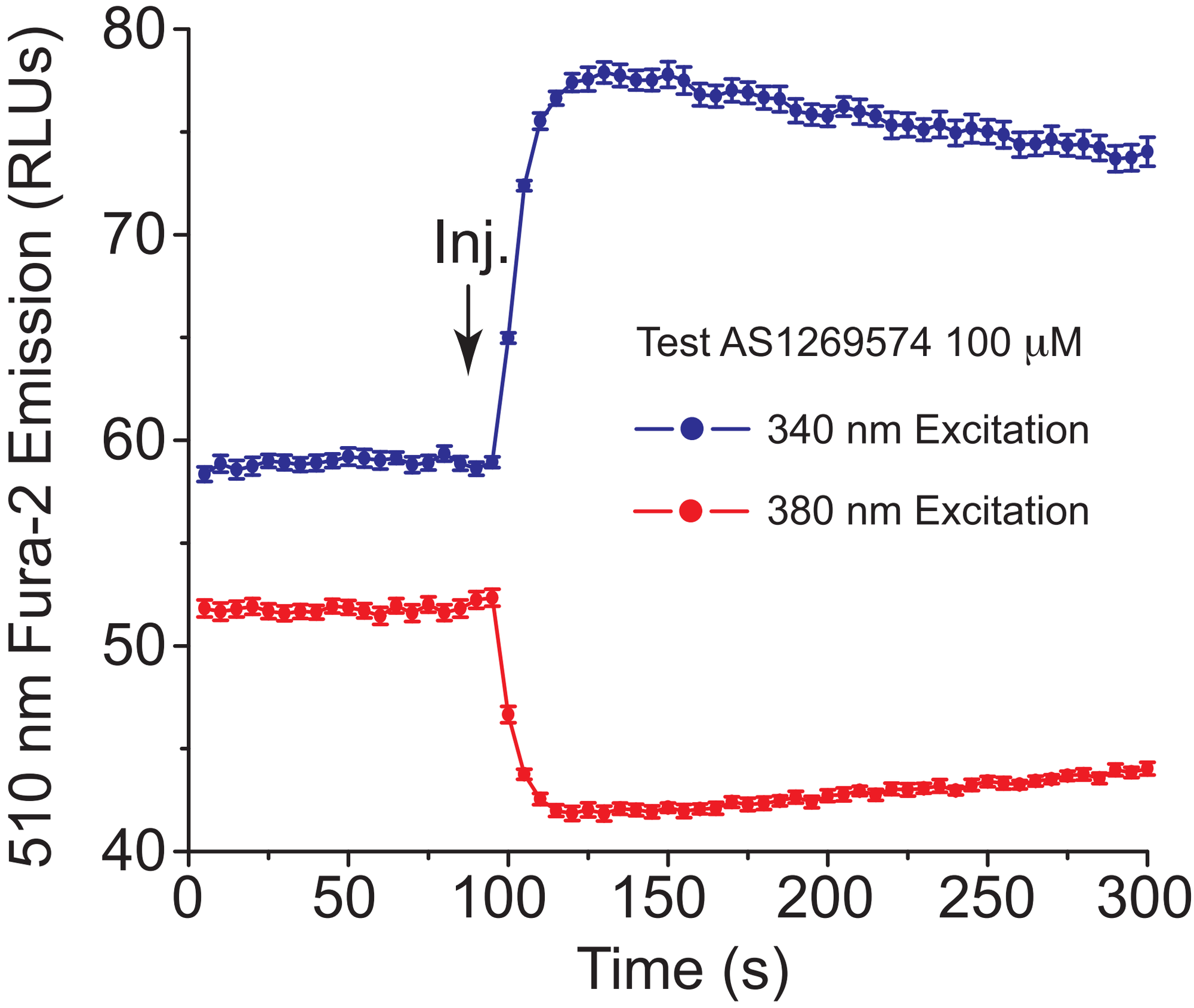

Supplemental Fig.S3

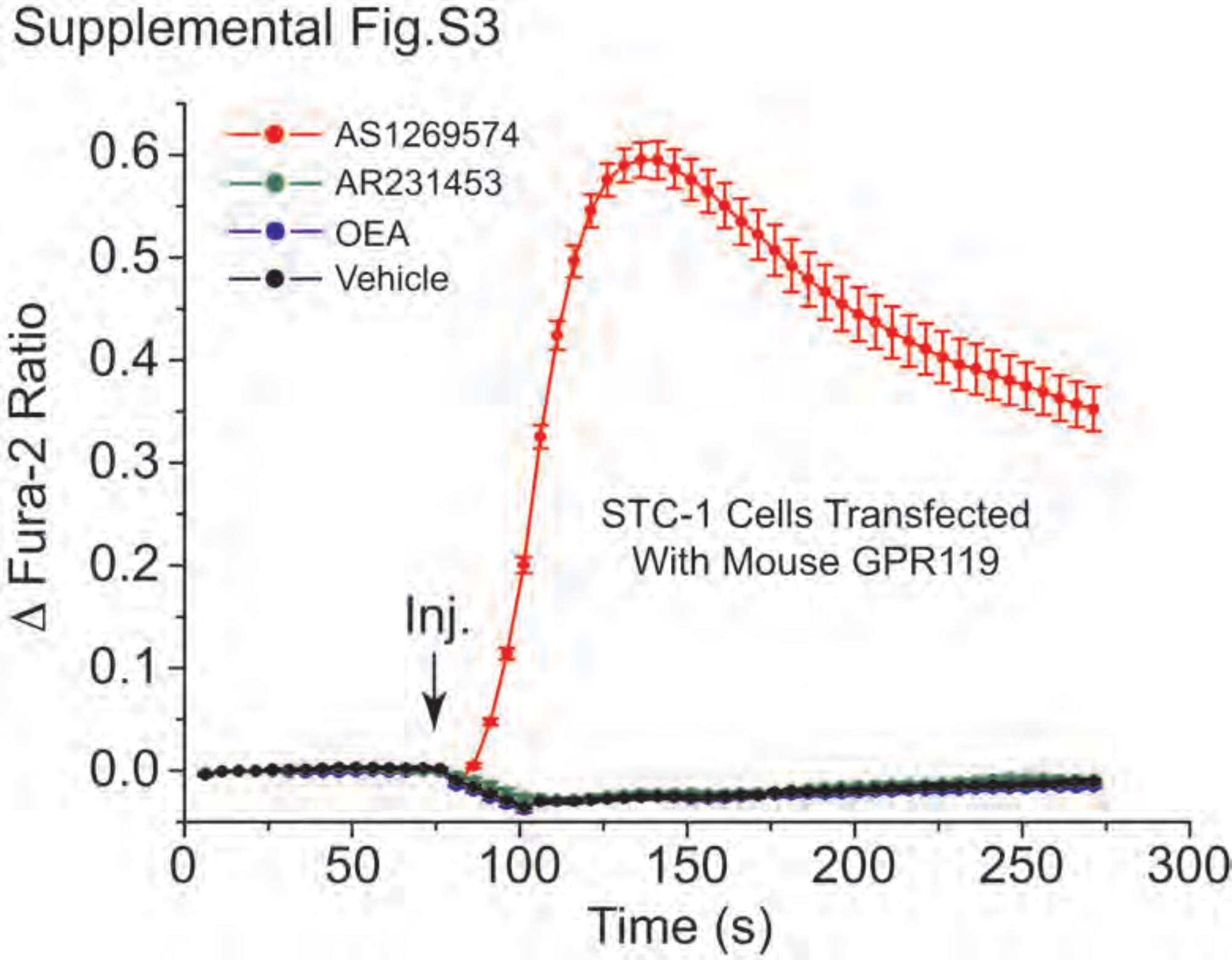

Supplemental Fig.S4

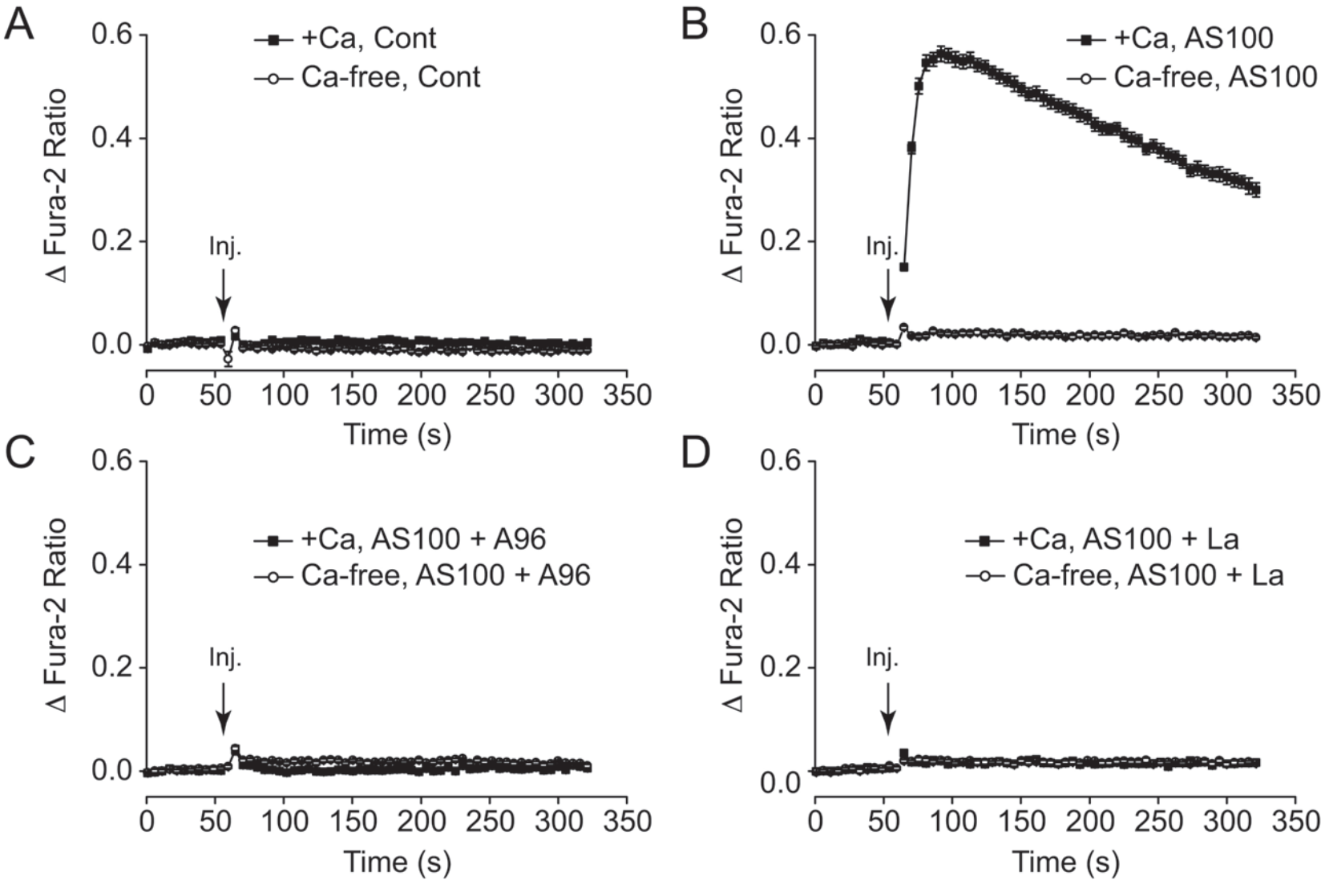

Supplemental Fig.S5

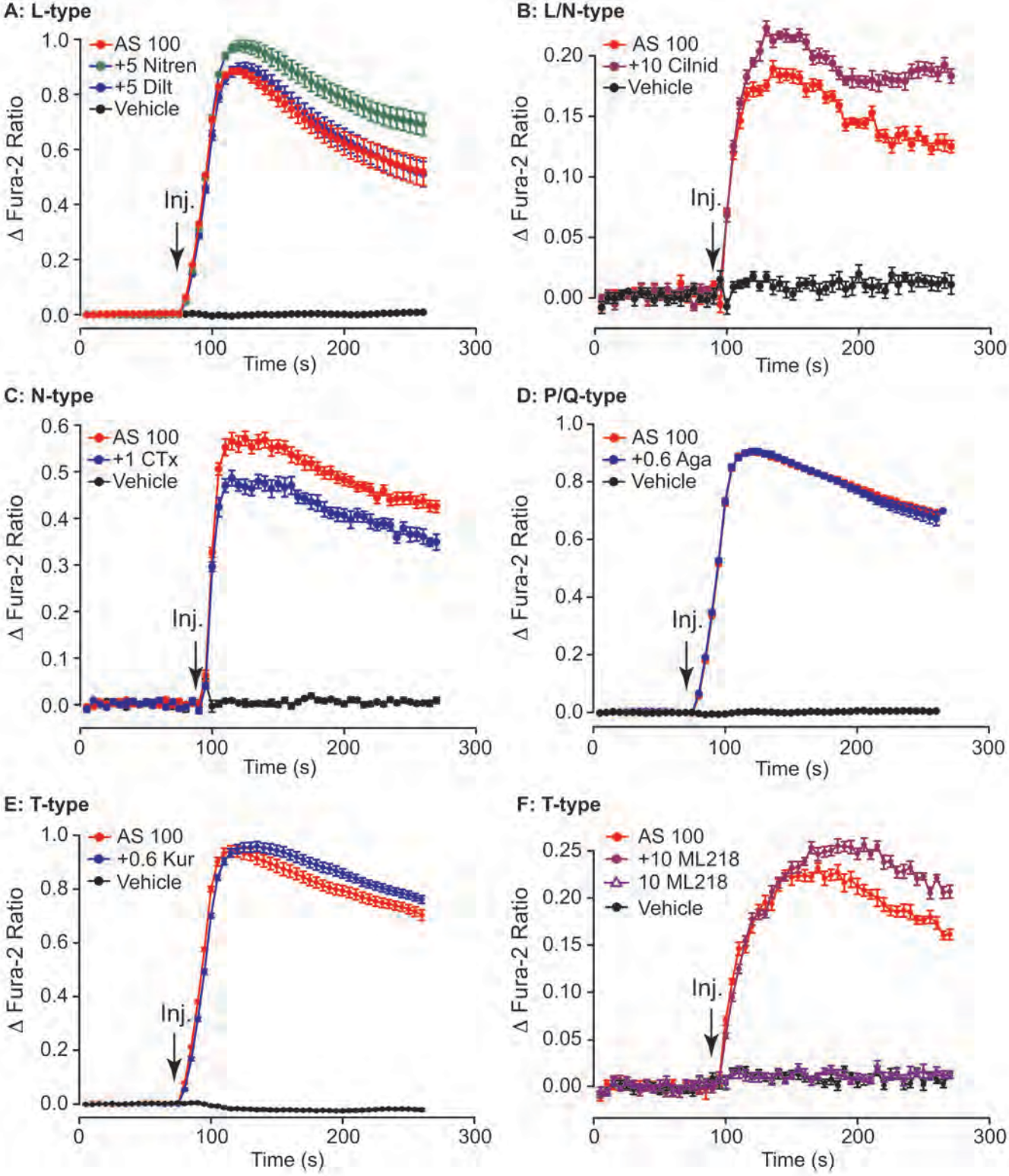

Supplemental Fig.S6

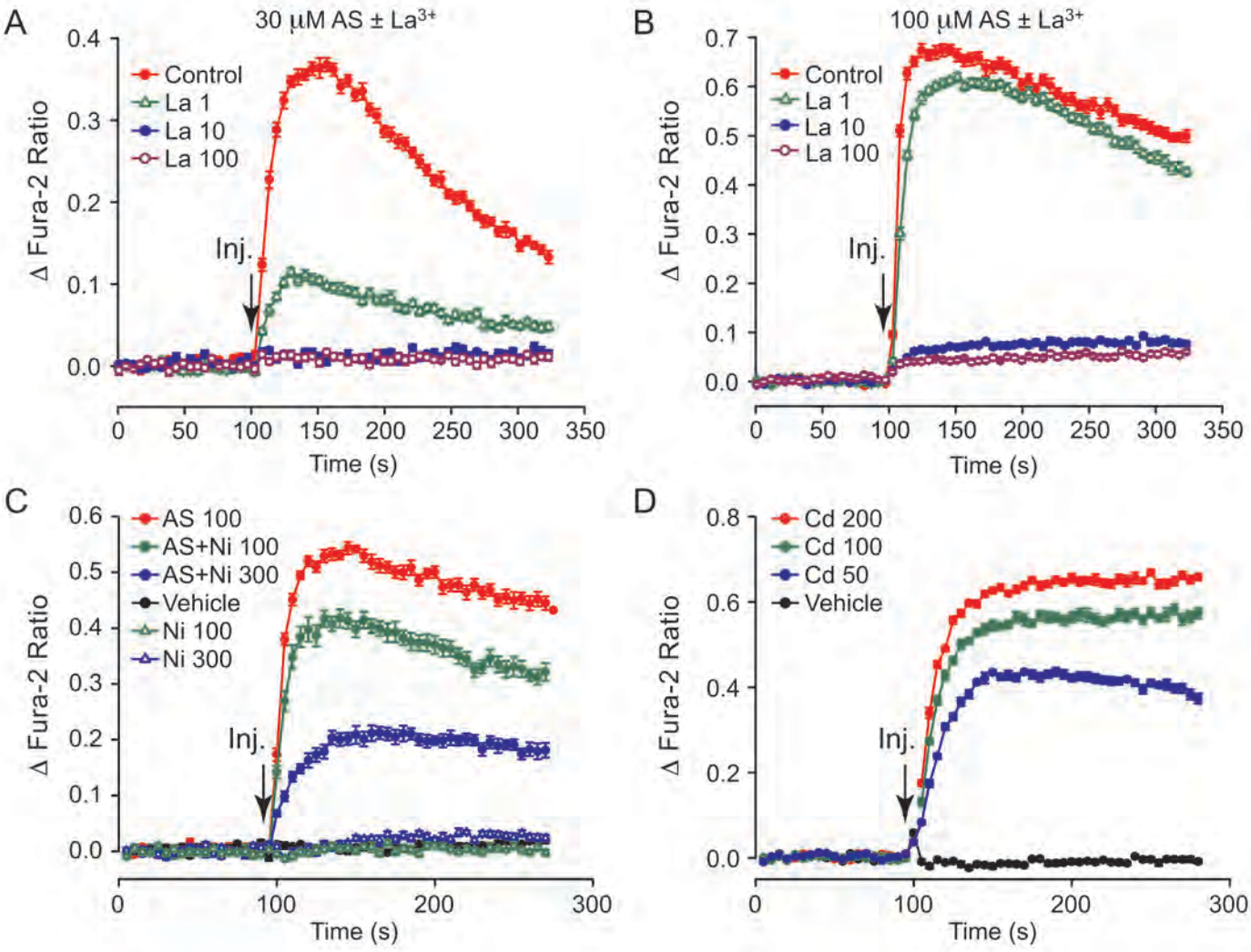

Supplemental Fig.S7

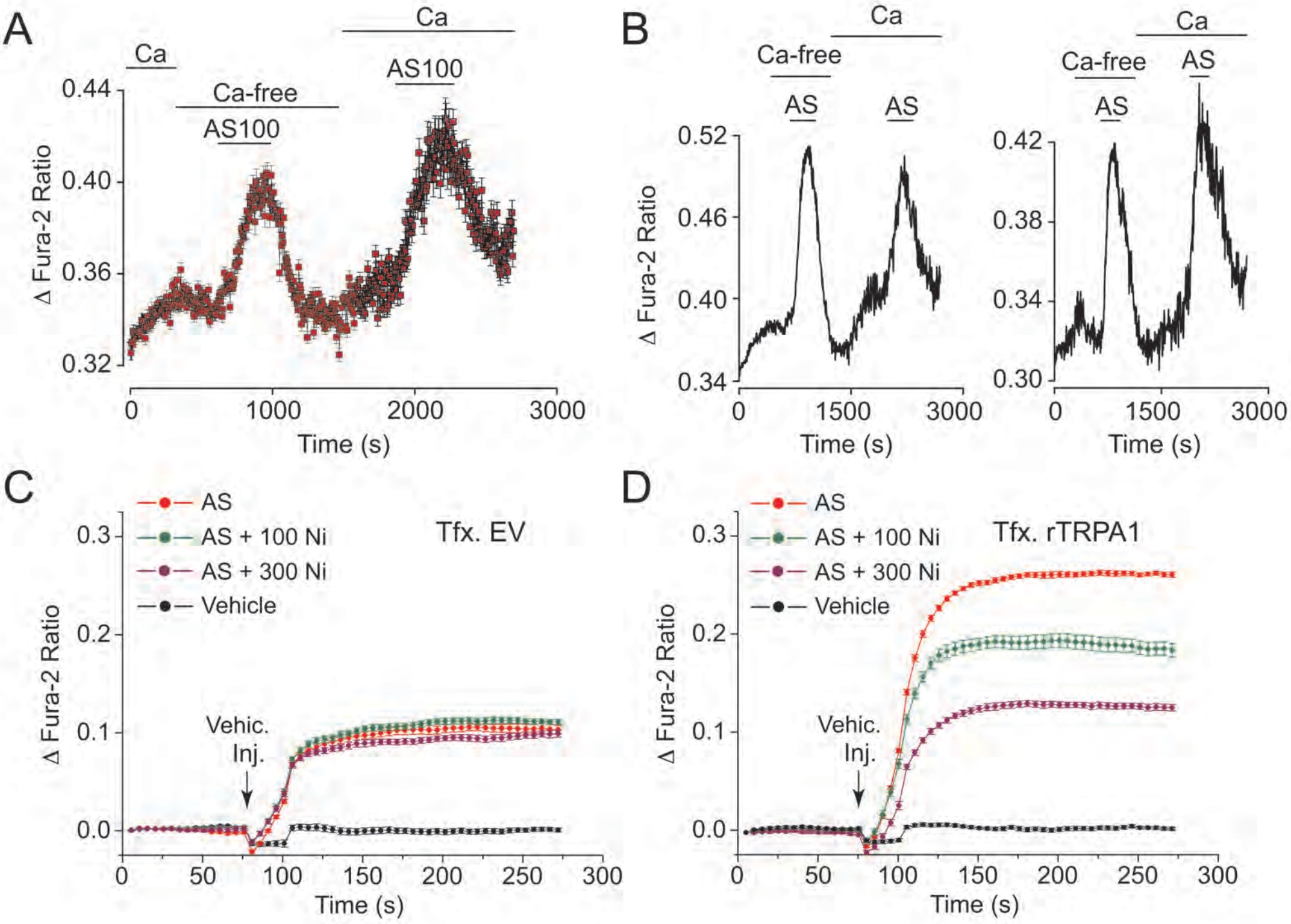

Supplemental Fig.S8

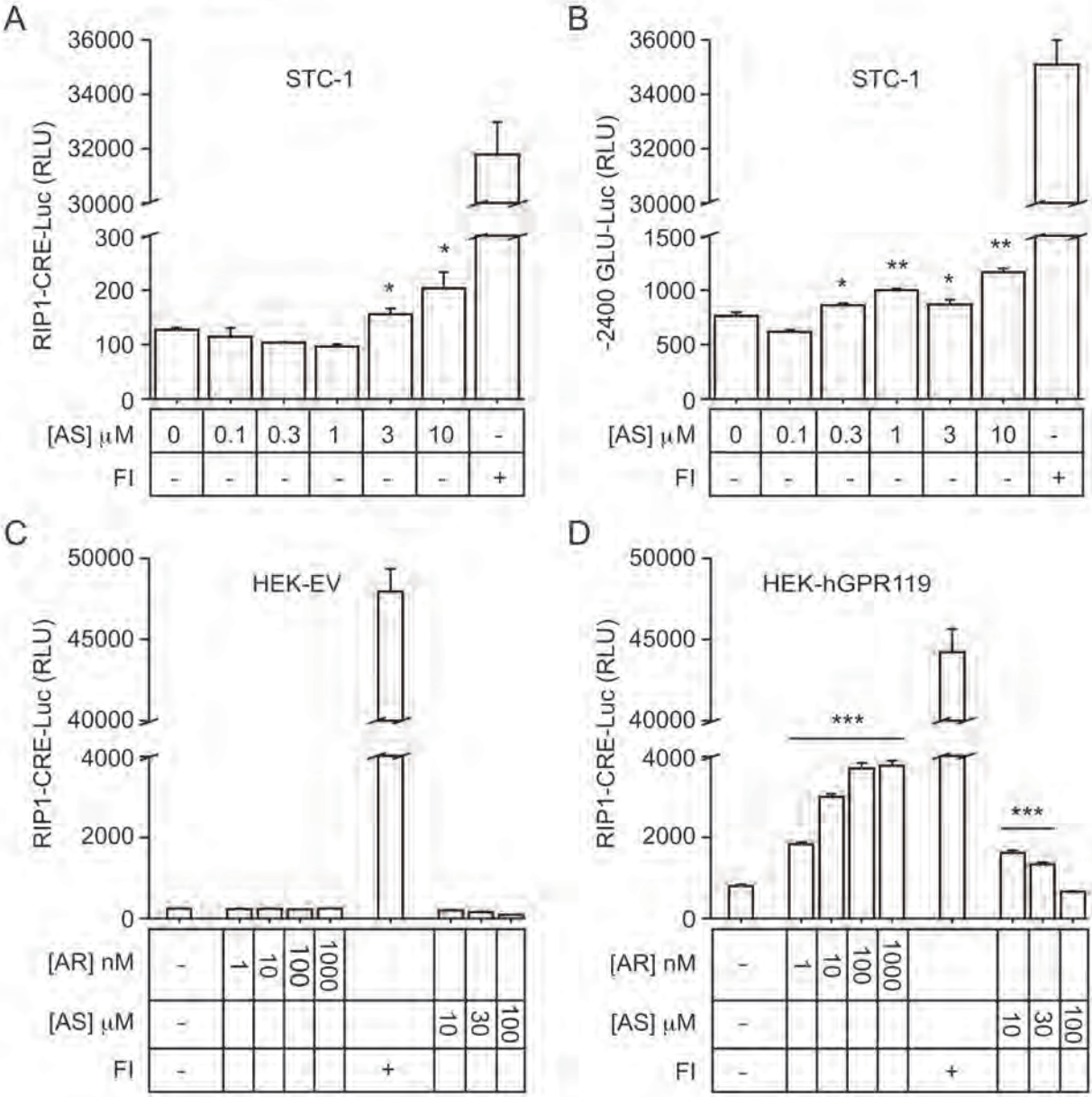

Supplemental Fig.S9

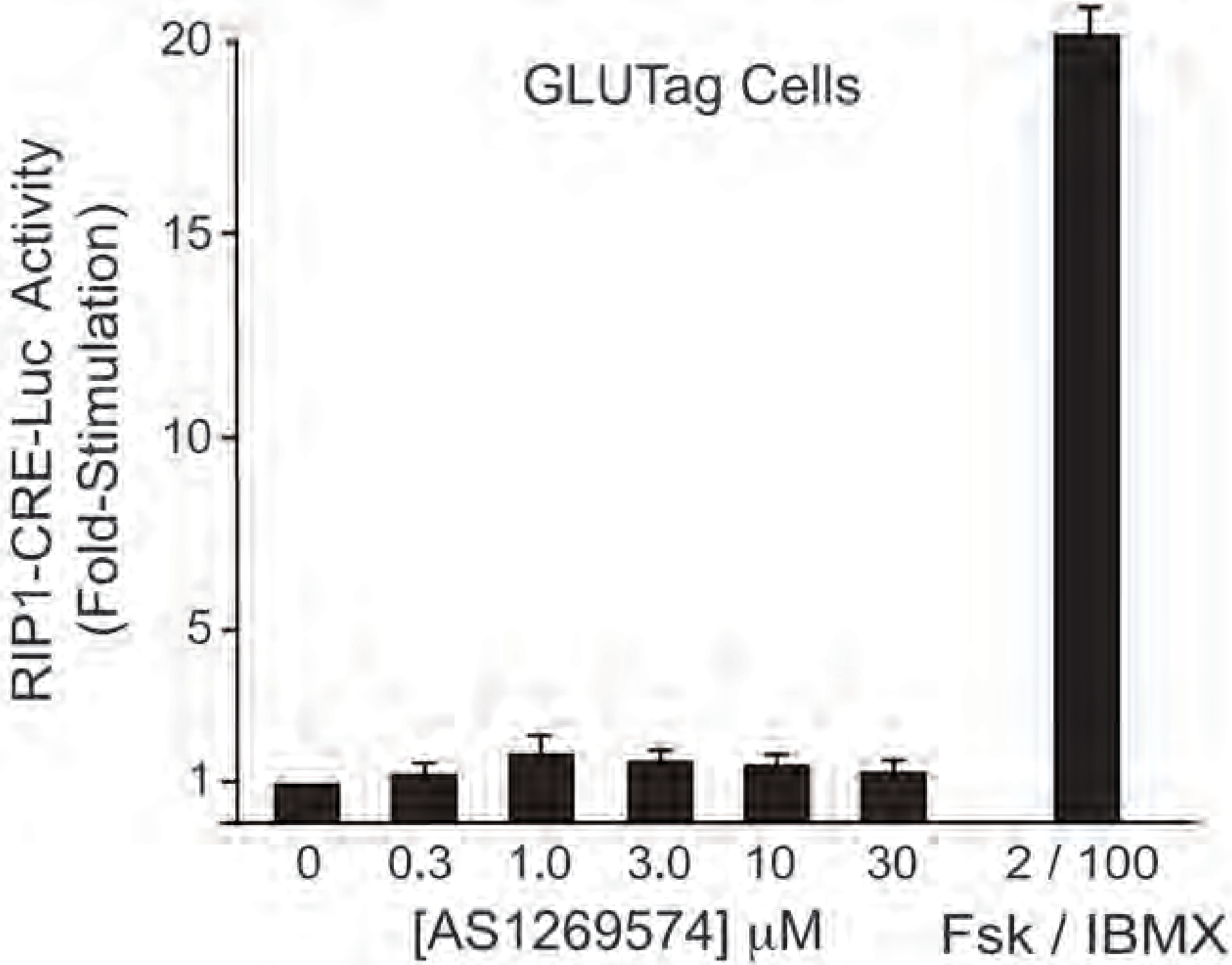

SUPPLEMENTAL MATERIAL

GPR119 agonist AS1269574 activates TRPA1 cation channels to stimulate GLP-1 secretion

***Oleg G. Chepurny[1], *George G. Holz[1,2], Michael W. Roe,[1,3] Colin A. Leech[1,4]**

Departments of Medicine[1], Pharmacology[2], Cell and Developmental Biology[3]
State University of New York (SUNY)
Upstate Medical University, Syracuse, New York, USA, 13210

* These authors contributed equally to this work

Supplemental Figures and Figure Legends: 9

Supplemental Movie and Legend: 1

[1]Address Correspondence and Reprint Requests to:

Colin A. Leech, Ph.D.
Associate Professor of Medicine
State University of New York (SUNY) Upstate Medical University
IHP 4304 at 505 Irving Avenue
Syracuse, NY, 13210
Tel. 315-464-1560
Fax 315-464-1561
E-mail: leechc@upstate.edu

Supplemental Figure Legends

FIGURE S1. Structures of GPR119 agonist AS1269574 and GPR119 antagonist TM43718.

FIGURE S2. Fura-2 based assay for $[Ca^{2+}]_i$ in STC-1 cell monolayers.

STC-1 cells were loaded with fura-2 so that an increase of $[Ca^{2+}]_i$ could be detected as a reciprocal change of the raw 340 and 380 nm fura-2 fluorescence emission intensities measured in response to the injection (Inj.) of AS1269574 (100 μM final concentration) into individual wells of a 96-well plate. Abbreviation: RLUs, relative light units.

FIGURE S3. Transfection with GPR119 fails to reveal a Ca^{2+}-elevating action of GPR119 agonists.

STC-1 cells transfected with recombinant mouse GPR119 exhibited an increase of $[Ca^{2+}]_i$ in response to AS1269574 (100 μM) whereas AR231453 (6 μM), and OEA (30 μM) were without effect.

FIGURE S4. Evidence for TRPA1 channel-mediated Ca^{2+} influx stimulated by AS1269574.

A, Negative control (Cont) test solutions demonstrated that $[Ca^{2+}]_i$ in STC-1 cell monolayers was unaffected by simple administration (Inj.) of a standard extracellular saline (SES) solution that contained Ca^{2+} (+C, Cont) or that was nominally Ca^{2+}-free (Ca-free, Cont).

B, AS1269574 (AS, 100 μM) stimulated an increase of $[Ca^{2+}]_i$ in STC-1 cell monolayers under conditions in which the SES contained 2.6 mM Ca^{2+} (+Ca, AS100), whereas it was without effect under conditions in which the SES was nominally Ca-free (Ca-free, AS100).

C, TRPA1 channel blocker A967079 (100 μM) suppressed the action of 100 μM AS1269574 to increase $[Ca^{2+}]_i$ under conditions in which the SES contained 2.6 mM Ca^{2+} (+Ca, AS100+A96). As expected, no increase of $[Ca^{2+}]_i$ was measured in response to AS1269574 under conditions in which the SES was nominally Ca^{2+}-free while also containing A967079 (Ca-free, AS100+A96).

D, The action of 100 μM AS1269574 to increase $[Ca^{2+}]_i$ in STC-1 cells was abolished under conditions in which the SES contained 2.6 mM Ca^{2+} and also 10 μM La^{3+} (+Ca, AS+La). As expected, no increase of $[Ca^{2+}]_i$ was measured in response to AS1269574 under conditions in which the SES was nominally Ca^{2+}-free while also containing La^{3+} (Ca-free, AS100+La).

A-D, The nominally Ca^{2+}-free solution was comprised of SES in which Na^+ was substituted for Ca^{2+} while also including 10 μM of the Ca^{2+} chelator EGTA.

FIGURE S5. Blockers of voltage-dependent Ca^{2+} channels fail to significantly inhibit the action of AS1269574 to increase $[Ca^{2+}]_i$ in STC-1 cells.

A-F, The action of 100 μM AS1269574 (AS 100) was tested in the absence or presence of:

A, L-type channel blockers nitrendipine (5 μM, +5Nitren) or diltiazem (5 μM, +5Dilt).

B, L/N type channel blocker cilnidipine (10 μM, +10 Cilnid).

C, N-type blocker omega-conotoxin GVIA (1 μM, +1 CTx).

D, P/Q type channel blocker omega-agatoxin IVA (600 nM, +0.6 Aga).

E, T-type channel blocker kurtoxin (0.6 μM, +0.6 Kur).

F, T-type channel inhibitor ML218 (10 μM, +10 ML218).

FIGURE S6. Evidence that AS1269574 activates non-selective cation channels in STC-1 cells.

A + B, The action of AS1269574 (AS, 30 or 100 μM) to increase $[Ca^{2+}]_i$ was dose-dependently inhibited by 1, 10, and 100 μM extracellular La^{3+} (La).

C, The action of 100 μM AS1269574 (AS 100) to increase $[Ca^{2+}]_i$ was dose-dependently inhibited by 100 or 300 μM extracellular Ni^{2+} (Ni 100, Ni 300).

D, Application of extracellular Cd^{2+} at 50, 100 or 200 μM (Cd 50, 100, or 200) stimulated an apparent increase of $[Ca^{2+}]_i$.

FIGURE S7. Ca^{2+} mobilizing and Ca^{2+} influx-promoting actions of AS1269574 in HEK-293 cells.

A + B, AS1269574 (AS, 100 μM) retained its ability to stimulate a small increase of $[Ca^{2+}]_i$ in HEK-293 cells under conditions in which the SES was nominally Ca^{2+}-free (Ca-free SES). Illustrated are the average responses from *N = 36* cells in a population study (A), or for *N = 2* single cell responses (B). The nominally Ca^{2+}-free solution was comprised of SES in which Na^+ was substituted for Ca^{2+} while also including 10 μM of the Ca^{2+} chelator EGTA.

C, extracellular Ni^{2+} (Ni, 100 or 300 μM) failed to alter the action of AS1269574 (AS, 100 μM) to increase $[Ca^{2+}]_i$ in HEK-293 cells transfected with the control empty vector (Tfx. EV).

D, the action of AS1269574 (AS, 100 μM) to increase $[Ca^{2+}]_i$ was enhanced by transfection of HEK-293 cells with rat TRPA1 (Tfx. rTRPA1), and this action of AS1269574 was dose-dependently inhibited by extracellular Ni^{2+} (Ni, 100 or 300 μM).

C-D, illustrated are findings from the same experiment using cells transfected on the same day.

FIGURE S8 . Evaluation of cAMP-regulated gene expression in STC-1 and HEK-293 cells.

A + B, Comparison of RIP1-CRE-Luc (A) and -2400 bp GLU-Luc (B) reporter activities in STC-1 cells under conditions of a 4 hour stimulation with AS1269574 (AS, 0.1 - 10 μM) alone, or the combined administration of forskolin (F, 2 μM) and IBMX (I, 100 μM). **C + D,** Comparison of RIP1-CRE-Luc reporter activity in HEK-293 cells transfected with empty vector (EV) or human GPR119 (hGPR119). Cells were treated for 4 hours with AR231453 (AR, 1 - 1,000 nM) or AS1269574 (AS, 10, 30, or 100 μM) or a combination of forskolin (F, 2 μM) and IBMX (I, 100 μM). (* $p < 0.05$; ** $p < 0.01$; *** $p < 0.001$; paired *t* test.).

Continued on the following page -

FIGURE S9. AS1269574 fails to stimulate RIP1-CRE-Luc activity in GLUTag cells.

AS1269574 (0.3 - 30 μM; 4 hr treatment) was not an effective stimulator of RIP1-CRE-Luc activity in GLUTag cells, whereas a strong stimulatory effect was measurable in response to combined administration of forskolin (2 μM) and IBMX (100 μM).

Supplemental Movie Legend

SUPPLEMENTAL Movie. Live-cell imaging of STC-1 cell monolayers revealed the rapid and reversible action of bath-applied AS1269574 (100 μM) to increase $[Ca^{2+}]_i$. The time span during which AS1269574 was administered is indicated by the appearance and subsequent disappearance of the red box labeled "AS100". Washout of AS1269574 was achieved by superfusion with SES that did not contain AS1269574. Pseudocoloring of the images was used to depict the $[Ca^{2+}]_i$ as being low (blue), intermediate (green-yellow), or high (red).